Adaptive Equivalent Consumption Minimization Strategy with Rule-based Gear Selection for the Energy Management of Hybrid Electric Vehicles Equipped with Dual Clutch

IEEE Access
Multidisciplinary ⋮ Rapid Review ⋮ Open Access Journal

Received October 1, 2020, accepted October 13, 2020, date of publication October 19, 2020, date of current version October 29, 2020.

Digital Object Identifier 10.1109/ACCESS.2020.3032044

Adaptive Equivalent Consumption Minimization Strategy With Rule-Based Gear Selection for the Energy Management of Hybrid Electric Vehicles Equipped With Dual Clutch Transmissions

GUIDO RICARDO GUERCIONI, ENRICO GALVAGNO, ANTONIO TOTA, AND ALESSANDRO VIGLIANI, (Member, IEEE)
Department of Mechanical and Aerospace Engineering (DIMEAS), Politecnico di Torino, 10129 Turin, Italy
Corresponding author: Alessandro Vigliani (alessandro.vigliani@polito.it)

ABSTRACT Based on observations of the behaviour of the optimal solution to the problem of energy management for plug-in hybrid electric vehicles, a novel real-time Energy Management Strategy (EMS) is proposed. In particular, dynamic programming results are used to derive a set of rules aiming at reproducing the optimal gearshift schedule in electric mode while the Adaptive Equivalent Consumption Minimization Strategy (A-ECMS) is employed to decide the powertrain operating mode and the current gear when power from the internal combustion engine is needed. In terms of total fuel consumption, simulations show that the proposed approach yields results that are close to the optimal solution and also outperforms those of the A-ECMS, a well-known EMS. One of the main aspects that differentiates the strategy here proposed from previous works is the introduction of a model to use physical considerations to estimate the energy consumption during gearshifts in dual-clutch transmissions. This, together with a series of properly tuned fuel penalties allows the controller to yield results in which there is no gear hunting behaviour.

INDEX TERMS Adaptive equivalent consumption minimization strategy (A-ECMS), dual-clutch transmission (DCT), energy management strategy (EMS), hybrid electric vehicle (HEV).

I. INTRODUCTION

In response to the ever-increasing demand for reduced fuel consumption and pollutant emissions, the automotive industry's main response has been the electrification of powertrain systems ([1]). Previous research has indicated that efficient energy management in Hybrid Electric Vehicles (HEVs) is of fundamental importance in order to fully exploit the capabilities of such systems ([2], [3]).

In production vehicles, Energy Management Strategies (EMSs) must be causal since real-time implementation is required, implying that control actions are local in time. The decision on how to split power among onboard energy sources depends on the vehicle architecture, and other decisions may also be necessary, e.g., current engaged gear, Internal Combustion Engine (ICE) state, clutch states, etc. ([4]).

The associate editor coordinating the review of this manuscript and approving it for publication was Amjad Anvari-Moghaddam.

The optimal solution to the energy management problem in HEVs can be found through Dynamic Programming (DP), i.e., a numerical method to solve problems in which a sequence of interrelated decisions have to be taken ([5]). DP is the only optimal control technique capable of solving problems of any complexity level within the accuracy limitations imposed by the discretization of problem variables ([2]); thus it generates benchmark solutions for real-time implementable EMSs ([6]–[8]). In addition, the results obtained with DP can be analysed to extract rules that generate a control trajectory similar to that of the global optimal solution ([9], [10]). For this method to work, an extensive calibration of the designed set of rules is needed to ensure satisfactory results for a wide range of operating conditions ([11]). This approach has been successfully applied in literature for the energy management of HEVs ([6], [9], [10] and [12]). It should be noted that the main advantage of rule-based techniques lies in the fact that they are easy to implement and computationally cheap since

no explicit optimization is involved ([13]). However, this also implies that the solutions are necessarily sub-optimal ([2]).

In the field of real-time implementable model-based control methods, several research efforts have also been dedicated to the Equivalent Consumption Minimization Strategy (ECMS) ([14], [15]). This approach can be used during vehicle operation since it is based on the minimization of a predefined cost function at each time step. Even though ECMS was first introduced in [14] as a heuristic method derived from engineering intuition, it was later shown that under certain conditions it could be regarded as an implementation of Pontryagin's Minimum Principle (PMP) ([16]), i.e., ECMS is able to provide the optimal solution to the energy management of HEVs. However, this depends on giving the proper value to the equivalence factor at each time instant.

Considering that a real-time implementable strategy cannot assume the future driving conditions as known, an adaptation scheme for the equivalence factor should be used to adjust this value as driving conditions change. In literature, EMSs performing online adaptation are referred to as the Adaptive Equivalent Consumption Minimization Strategy (A-ECMS) ([17]–[19]). Several A-ECMS formulations have been proposed using a series of different techniques. For example, in [17] the best value of the equivalence factor is found by means of a receding-horizon optimization based on an estimation of the future driving conditions. Instead in [20], an algorithm for driving pattern recognition is employed, exploiting the fact that the optimal equivalence factor is similar for cycles with similar statistical properties,. Alternative formulations using feedback from the battery State Of Charge (SOC) have also been proposed: the idea is to dynamically update the value of the equivalence factor employing classical feedback control methods based on the difference between the current SOC and a predefined reference ([2]). This technique has been successfully implemented in [21] for a charge-sustaining HEV and in [4] for a Plug-in Hybrid Electric Vehicle (PHEV). It should be noted that the main practical implementation issue of such adaptation schemes lies on providing a suitable reference for the SOC. For charge-sustaining operation, the SOC reference is usually regarded as a constant ([21]). Instead, for charge-depleting operation, like that generally seen in PHEVs, the optimal SOC trajectory has been found to be approximately a quasi-linear decreasing function of the travelled distance, which in literature is referred to as a blended strategy ([22]–[24]). Finally, in order to properly initialize the equivalence factor, a pre-computed offline map can be used in which the optimal values are stored for several different cycles based on the total travelled distance and the average speed [4].

Due to their formulation, instantaneous minimization methods are inclined to provide control requests that generate high frequency switching between operating points. The reason is that the cost related to different control candidates may be very similar; hence, small variations in the driving conditions can lead to continuously select different operating points based on negligible improvements in the cost function of interest. When fuel consumption is the main concern, the request of transient events such as gearshifts and ICE starts that would result in negligible improvement should be avoided since, in addition to the associated energy losses, drivability issues would also arise ([25], [26]).

Dual-clutch transmissions (DCTs) can deliver the power from the engine to the output shaft smoothly during the shift process without power interruption ([27], [28]), leading to high transmission efficiency and reducing the energy loss. Therefore, the combination of PHEVs and DCTs can reduce fuel consumption, reduce pollutant emissions and improve drivability [29]. Modelling of energy consumption during gearshifts and ICE starts is a fundamental aspect that differentiates the real-time implementable EMSs developed here from the DP formulations as presented in [30]. One solution involves an additional weighting factor to the DP algorithm cost function for gearshifts and/or ICE starts events as described in [31] and [25]. A more accurate approach consists of including a physical DCT gearshift model as described in [32] and an ICE start model as provided by [33] but applied to an Automated Manual Transmission (AMT).

To the best of the authors' knowledge, no EMS is yet available in which physical considerations are used to model energy consumption during both gearshifts and ICE starts for Dual-Clutch Transmissions. Well-designed modelling of the power losses during these transient events together with a series of properly tuned fuel penalties allows the controller to yield results without gear hunting or chattering in the ICE state. The contribution of this article aims at filling this gap with a causal EMS whose design includes the energy consumption during gearshifts and ICE starts. A causal EMS is designed in which DP results are used to derive a set of rules aiming at reproducing the optimal gearshift schedule in EV-mode; at the same time, an A-ECMS formulation with a discrete adaptation scheme based on SOC feedback ([4]) is employed to decide the powertrain operating mode (through the torque split factor) and the current gear when power from the ICE is needed. The novel algorithm, here named RB + A-ECMS, proposes a rule-based gear selection in EV-mode integrated with an A-ECMS formulation.

Simulation results show that, in terms of total fuel consumption, the proposed approach not only yields results close to the optimal solution but also outperforms those of the A-ECMS, a well-known EMS.

The present paper is organized as follows. In section II, the structure and capabilities of the PHEV are addressed together with the model of its powertrain to account for the energy consumption during gearshifts and ICE starts. Then, the optimal control problem formulation is given. In section IV, a complete overview of the algorithm is provided in which the main inputs and outputs are described. The section also presents some considerations based on the behaviour of the optimal solution from which the principle behind the proposed approach is extracted. Section V discusses each algorithm phase. In the following two sections, the proposed A-ECMS formulation is described in detail and the rule-extraction

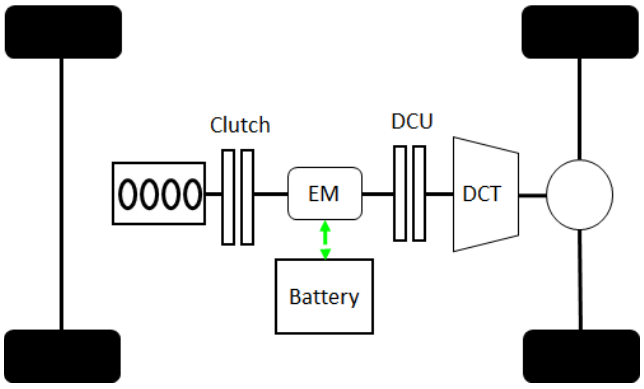

FIGURE 1. Powertrain layout.

TABLE 1. Powertrain components specifications.

Component	Data
Vehicle mass	1520 kg
ICE	Gasoline engine, 1.4 L, 110 kW
EM	75 kW (peak power)
DCT	6-speed transmission
Battery Pack	Li-ion, 8.8 kWh (26.5 Ah)

process from DP results is illustrated. Finally, simulation outcomes are presented and analysed in section VIII.

II. POWERTRAIN DESCRIPTION AND MODELLING

A. POWERTRAIN DESCRIPTION

The vehicle under analysis is equipped with a parallel PHEV architecture, as visible in Fig. 1. The powertrain consists of an ICE, an Electric Machine (EM), a battery pack and a DCT.

The ICE and the EM are mounted on the same shaft, which is connected to the transmission input through the Dual-Clutch Unit (DCU). Hence, to propel the vehicle, it is possible to use the two motors together or separately. It should be noted that the ICE could produce additional power, with respect to what strictly required at the wheels, to recharge the battery through the EM, acting as a generator.

As typical for hybridized powertrains, the introduction of the EM enables the possibility of performing regenerative braking.

A quick-disconnect dry clutch allows to separate the ICE from the rest of the powertrain when needed. This feature is particularly attractive when the powertrain operates in EV-mode since it allows the EM to propel the vehicle without dragging the ICE inertia, thus reducing energy losses.

Table 1 shows the most relevant specifications for the powertrain components.

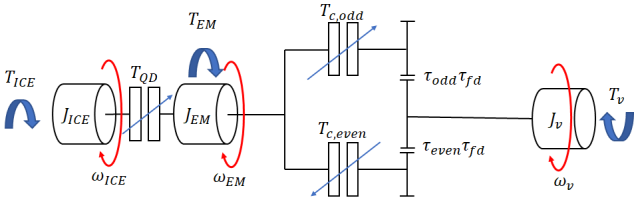

FIGURE 2. Powertrain model: gearshifts energy request.

B. POWERTRAIN MODEL

The backward quasi-static model presented in [30] is used here for the development and testing of the proposed EMS; therefore, it will not be described in detail in this work.

As stated in the introduction, one fundamental aspect that differentiates the real-time implementable EMS developed here from those published in previous works, is the integration of the model of the energy consumption during gearshifts and ICE starts, into the optimal control problem formulation. Appropriate modelling of the power losses during these transient events assists the controller in avoiding undesirable gear hunting behaviour and chattering in the ICE state.

The estimation of the energy losses associated to gearshifts and ICE starts relies on a powertrain model, thus allowing to quantify the energy dissipation related to several solution candidates to the energy management problem, without considerably increasing the computational effort. The powertrain model is shown in Fig. 2, where J_{ICE}, J_{EM} and J_v represent the ICE, the EM and the equivalent vehicle inertia respectively.

It should be noted that since the HEV of interest is not equipped with a conventional starter, during engine starts the crankshaft needs to be accelerated by the torque passing through the quick-disconnect clutch until the ICE minimum firing speed is reached.

The speed profiles of the ICE (ω_{ICE}), EM (ω_{EM}) and the two clutches ($\omega_{c,odd}$, $\omega_{c,even}$) together with each clutch transmissible torque profile are assumed to be known inputs for the expressions presented in this section. Simplified linear profiles of speed and torque are assumed accordingly to the characteristics of the simulated manoeuvres and the vehicle states (see [30] for more details). T_v represents the equivalent vehicle coast-down resistance torque and ω_v is the equivalent vehicle speed.

In the developed model, when the quick-disconnect clutch is not engaged, the ICE and EM dynamics are described by:

$$J_{ICE}\dot{\omega}_{ICE}(t) = T_{ICE}(t) - T_{QD}(t) \quad (1)$$

$$J_{EM}\dot{\omega}_{EM}(t) = T_{EM}(t) + T_{QD}(t) - T_c(t) \quad (2)$$

Instead, when the quick-disconnect clutch is engaged, it holds:

$$(J_{ICE} + J_{EM})\,\dot{\omega}_{EM}(t) = T_{EM}(t) + T_{ICE}(t) - T_c(t) \quad (3)$$

where $\dot{\omega}_{EM}(t) = \dot{\omega}_{ICE}(t)$.

In the previous equations, $T_{ICE}(t)$ and $T_{EM}(t)$ are respectively the ICE and EM net torque; $T_{QD}(t)$ is the torque

being transmitted by the quick-disconnect clutch. Moreover, the total torque $T_c(t)$ passing through the DCU and the torque applied to the wheels $T_w(t)$ can be written as:

$$T_c(t) = T_{c,even}(t) + T_{c,odd}(t) \quad (4)$$

$$T_w(t) = T_{c,even}(t)\,\tau_{tot,even}(t) + T_{c,odd}(t)\,\tau_{tot,odd}(t) \quad (5)$$

with

$$\tau_{tot,even}(t) = \tau_{even}(t)\,\tau_{fd} \quad (6)$$

$$\tau_{tot,odd}(t) = \tau_{odd}(t)\,\tau_{fd} \quad (7)$$

where, $T_{c,even}(t)$ and $T_{c,odd}(t)$ are the torque passing by the offgoing and oncoming clutch, respectively. Accordingly, $\tau_{even}(t)$ and $\tau_{odd}(t)$ are the transmission ratios of the even and odd gears transmission shafts; τ_{fd} is the final drive gear ratio. It should be noted that the transmissible torque profiles for the gearbox clutches are computed in order to satisfy the torque request at the wheels.

From the power equilibrium at the clutches, the following expressions are found:

$$T_{c,even}(t)\omega_{EM}(t) = T_{c,even}(t)\omega_{c,even}(t) + P_{c,even,loss}(t) \quad (8)$$

$$T_{c,odd}(t)\omega_{EM}(t) = T_{c,odd}(t)\omega_{c,odd}(t) + P_{c,odd,loss}(t) \quad (9)$$

$$T_{QD}(t)\omega_{ICE}(t) = T_{QD}(t)\omega_{EM}(t) + P_{QD,loss}(t) \quad (10)$$

It should be noted that in the former equations when $\omega_{EM}(t) \neq \omega_{c,even}(t)$, or $\omega_{EM}(t) \neq \omega_{c,odd}(t)$, or $\omega_{EM}(t) \neq \omega_{ICE}(t)$ a certain amount of energy is dissipated.

Hence, $P_{QD,loss}(t)$, $P_{c,even,loss}(t)$ and $P_{c,odd,loss}(t)$ represent the slip power losses for each clutch. Therefore, through physical considerations, this simplified model allows accounting for these dissipations, together with the energy needed for the powertrain components to follow the requested speed profiles during gearshifts and ICE starts. The effectiveness of the models in estimating the overall energy request to undertake these transient manoeuvres is studied in detail in [30], where it is shown that for the optimal solution obtained with DP, when both sources of losses are considered within the optimal control formulation, there is no gear hunting or chattering. Furthermore, simulations over three repetitions of the WLTC class 3, version 3.2 [36] during charge-sustaining vehicle operation (50% SOC target) present a reduction above 200% in the overall number of gearshifts and ICE starts with respect to the case in which no losses for these events are accounted for.

Fig. 3 provides an example, for an upshift, of how the energy necessary to undertake the gearshift process is distributed. It can be appreciated that the amount of energy dissipated in clutch slip, is not negligible. Moreover, it should be noted that the need to decrease the speed of the EM shaft helps reducing the total requested energy.

Similarly to the gearshift results, the energy dissipation due to clutch slip is not negligible during ICE starts as it can be appreciated in the example shown in Fig. 4.

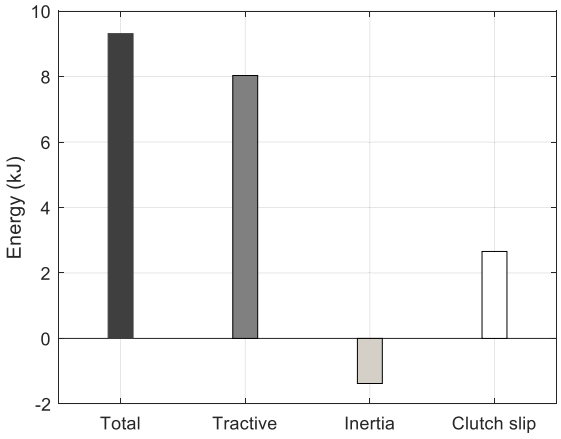

FIGURE 3. Gearshift energy distribution: upshift.

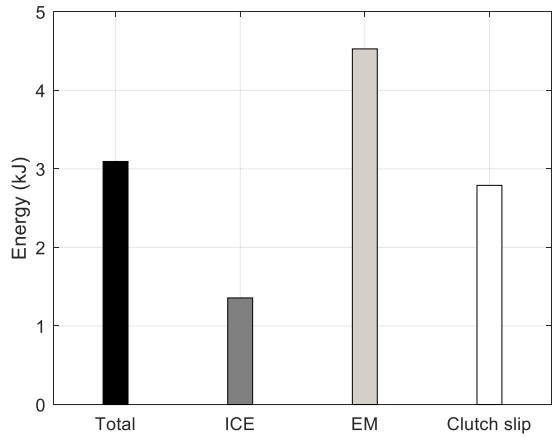

FIGURE 4. ICE start energy.

III. OPTIMAL CONTROL PROBLEM FORMULATION

The energy management of the PHEV is cast into a constrained finite time optimal control problem. It consists in finding the control law that minimizes a predefined performance index while meeting the dynamic state constraints, the local and global state constraints and the local control constraints ([2]).

Similar to [30], state x_k and control u_k variables have to be defined, bounded and discretized.

In addition, the powertrain model must be expressed as a discrete-time system:

$$x_{k+1} = f_k(x_k, u_k) \quad (11)$$

Equation (11) represents the dynamic state constraints of the problem, where k takes integer values and indicates the current time step $t = kT_S$ (the duration of each computation step T_S is 1 s).

Local constraints are also defined:

$$x_k \in X_k \quad (12)$$

$$u_k \in U_k \quad (13)$$

where X_k and U_k are respectively the states and controls domains.

Furthermore, also global state constraints need to be considered, to enforce a desired final value x_{tgt} or an acceptable range Δx around it for state variables:

$$x_N - x_{tgt} = \pm \Delta x \tag{14}$$

Once defined a discrete representation of the system together with its boundaries, a suitable cost function is needed to fully describe the optimal control problem. Let us consider a generic performance index, given as a function of the initial states x_0 and control law u:

$$\Psi(x_0, u) = \sum_{k=1}^{N} L_k \tag{15}$$

where L_k is the instantaneous cost function and N indicates the final time step counter.

A. COST FUNCTION

The optimal control problem consists of minimizing the overall fuel consumption during a certain driving mission. The instantaneous cost function is defined as

$$L_k = \dot{m}_{f,t,k} \tag{16}$$

To account for the fact that the ICE will cool down during the time steps in which the quick-disconnect clutch is disengaged and the engine is off, a fuel penalty is introduced to account for the extra quantity of fuel that has to be used. For simplicity, a constant value is considered. Finally, the total fuel consumption rate $\dot{m}_{f,t,k}$ is:

$$\dot{m}_{f,t,k} = \begin{cases} \dot{m}_{f,k} + \dot{m}_{f,cds}, & if\ es_k = 1 \\ \dot{m}_{f,k}, & otherwise \end{cases} \tag{17}$$

where $\dot{m}_{f,k}$ is interpolated from the ICE fuel rate map as a function of angular speed and torque request, which through physical models considers the energy consumed to bring the ICE to the target speed during start manoeuvres and gearshifts (see [30] for further details). Instead, $\dot{m}_{f,cds}$ is the fuel penalty for ICE cold starts (0.1 g/s). Some reference values for the energetic cost of engine start can be found in [39].

It should be noted that when the ICE state goes from 0 to 1, i.e., from off to on, the ICE start status es_k is set to 1, otherwise, it is set to 0.

B. STATES AND CONSTRAINTS

Four state variables are defined together with a series of local and global state constraints as described in the following paragraphs.

1) SOC

The dynamics of the battery SOC is given by:

$$SOC_k = SOC_{k-1} - \frac{I_k}{Q_{nom}} T_s \tag{18}$$

where Q_{nom} is the battery nominal capacity. The battery current I_k is computed using a control-oriented zero-th order equivalent circuit model ([35]).

The estimation of the SOC value at each iteration enables the control algorithm to account for the physical limitations of the energy storage system and to impose a final target. The maximum value of the SOC depends on the characteristics of the energy storage system. To account for the fact that the proposed real-time implementable EMS cannot guarantee to achieve the exact value required at the end of the cycle $SOC_{ref,N}$ (the global state constraint), which is common for most ECMS-based approaches ([2]), a 1% variation below the desired value is considered acceptable. Hence, the local state constraints are defined as: $SOC_k \in [SOC_{ref,N} - 0.01, 0.93]$.

2) GEAR NUMBER

In order for the EMS to account for the energy consumption of gearshift manoeuvres, which is computed as described in [30], the gear number $gn_{x,k}$ is defined as a state. Each time there is a variation in the gear number state, the gearshift status gs_k becomes 1 (otherwise 0) and the mentioned power losses are computed.

The state dynamics depends only on the control inputs, i.e., $gn_{x,k} = gn_{u,k}$, where $gn_{u,k}$ is the gear command.

Since the PHEV under analysis is equipped with a 6-speed DCT, seven discrete values are possible for the gear number state: $gn_{x,k} \in [0, 6]$. The neutral gear ($gn_{x,k} = 0$) is forced when the torque request to the vehicle is zero. The reverse gear is not considered in this analysis.

3) ICE STATE

Differently from the work presented in [30], the fuel cut-off functionality is not considered here for practical implementation reasons. This means that if the quick-disconnect clutch is engaged, the ICE is either being used to supply for the power request at the wheels (or part of it) or to recharge the battery.

As it can be inferred from the previous remarks, the ICE state is a binary variable that can assume one of two values: off ($ICE_{x,k} = 0$) or on ($ICE_{x,k} = 1$).

The ICE state is determined by the torque request resulting from the torque split control input (see section III.C):

$$ICE_{x,k} = \begin{cases} 1, & if\ T_{ICE,k} > 0 \\ 0, & otherwise \end{cases} \tag{19}$$

where $T_{ICE,k}$ is the torque request to the ICE decided by the EMS.

It should be noted that since each time the ICE is turned off and the quick-disconnect clutch is opened, an ICE start event will be necessary the next time engine propulsion will be reapplied. This implies that the ICE state variable must be defined in order for the EMS to consider the ICE start losses (see [30]). In this way, by comparing the value of this variable at the previous iteration with the command being given at the current step, ICE start manoeuvres are detected, and the corresponding losses can be estimated.

4) EM TORQUE COUNTER STATE

A counter is needed to establish whether to enforce the continuous or peak torque limit when defining the set of admissible control inputs to the EM. From experimental experience, it was determined that if the continuous torque limit is breached for 7 consecutive seconds, at least 13 s must pass before the EM torque can go again above its continuous boundary. This condition is set to ensure that the EM components operate in the desirable temperature range.

Hence, a counter is designed so that each time the torque request is within the continuous limit and counter value is lower than 7, a reset is enforced. On the other hand, when the counter reaches a value of 7, it is reset only after 13 additional time steps have passed.

Based on the previous considerations, the following local conditions are established: $T_{EM,lim,k} \in [0, 20]$. It should be noted that the range of admissible values is given in terms of time steps to be able to enforce the limitations discussed above.

C. CONTROLS AND CONSTRAINTS

In the following, the physical meaning of each control variable is addressed, and the local control constraints are reported.

1) TORQUE SPLIT FACTOR

The Torque Split Factor (TSF) is a control variable introduced to indicate how the total power request at the wheels is distributed between the powertrain actuators, i.e. ICE and the EM. It is defined as the ratio between the EM torque request $T_{EM,k}$ and the total torque request at the transmission input $T_{t,k}$:

$$TSF_k = \frac{T_{EM,k}}{T_{t,k}} \tag{20}$$

The local constraints on the TSF are: $TSF_k \in [-1, 1]$.

Given the definition presented in (20), the physical meaning of the values the TSF can take is:

- $TSF_k = 1$ implies operation in EV-mode;
- $TSF_k \in (0, 1)$ implies operation in parallel hybrid mode;
- $TSF_k = 0$ implies operation in ICE-only mode;
- $TSF_k \in [-1, 0)$ implies operation in hybrid mode. In this case, additional torque, with respect to the torque requested for traction, is supplied by the ICE to recharge the battery and/or optimize its operating point. In theory, the amount of torque available to recharge the battery is only bounded by the physical limitations of powertrain components. For the simulations presented, the value of -1 is used, implying that the torque available for battery recharge can be high as the one requested to satisfy the wheel torque request. It is worth mentioning that the lower boundary of the TSF was only reached in few situations in the simulations performed to find the optimal energy management strategy as reported in [30].

2) GEAR COMMAND

At each time step, the EMS must select the engaged gear: there are six possible gears to choose from: $gn_{u,k} \in [1, 6]$.

3) QUICK-DISCONNECT CLUTCH COMMAND

The quick-disconnect clutch command depends, as explained in section III.B, on the power request to the ICE. This control is a binary variable:

- $QD_{u,k} = 1$ implies that the clutch must be closed or kept closed;
- $QD_{u,k} = 0$ implies that the clutch must be opened or kept open.

4) INSTANTANEOUS CONSTRAINTS

During vehicle operation, a series of constraints must be enforced to ensure that the physical limits of the powertrain actuators are respected when elaborating the control output signals. Since the PHEV here analysed corresponds to that studied when developing the DP formulation presented in [30], the same conditions are defined:

$$\begin{aligned} P_{b,min,k} &< P_{b,k} < P_{b,max,k} \\ \omega_{j,min} &< \omega_{j,k} < \omega_{j,max} \\ T_{j,min,k} &< T_{j,k} < T_{j,max,k} \end{aligned} \tag{21}$$

with j being a generic index that in this case stands for either ICE or EM.

IV. ALGORITHM OVERVIEW

The global control scheme used for the analysis is illustrated in Fig. 5.

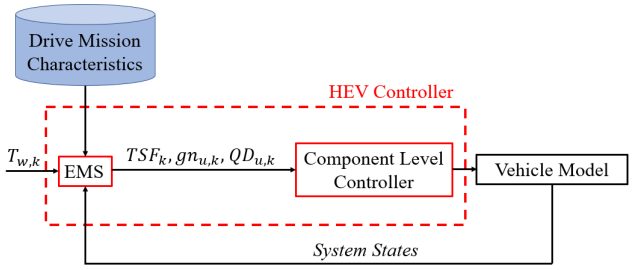

FIGURE 5. General control scheme.

The HEV controller is sub-divided into two control modules: EMS and the Component Level Controller. At each time step, the EMS module decides the vehicle operating mode through the selection of the TSF, the quick-disconnect clutch command and the gear number. This decision is based on the torque request at the wheels T_w (computed accordingly to the adopted backward quasi-static modelling approach), some a-priori information regarding the mission characteristics and the current system states coming from the vehicle model. This information is then passed to the component level controllers to determine the powertrain actuators setpoints (typical examples for component level controllers are provided in [37]–[39]). It should be noted that the mentioned vehicle

model is used both to assess the effects of the control decisions made by the EMS on the system states and for their generation. As explained before, model-based control methods, rely on suitable models of the system to test several solution candidates at each iteration [4].

The EMS proposed here is developed from a detailed analysis of the optimal solution behaviour. After performing several simulations using the DP formulation developed in [30], it was observed that the gearshift schedule obtained when increasing the value of the final SOC target, thus forcing a more charge-sustaining operation, can be interpreted as the one obtained when the vehicle operates in EV-mode with some deviations. The mentioned deviations correspond most times to gearshifts performed when the intervention of the ICE is required. This can be clearly seen in Fig. 6, comparing the optimal gear number state trajectory in EV-mode (labelled "free SOC_N" in the legend) with HEV-mode resulting from the request of the final SOC to be 75%. The driving cycle considered is the WLTC class 3, version 3.2 ([36]). All the driving cycles studied in this article are shown in Appendix II.

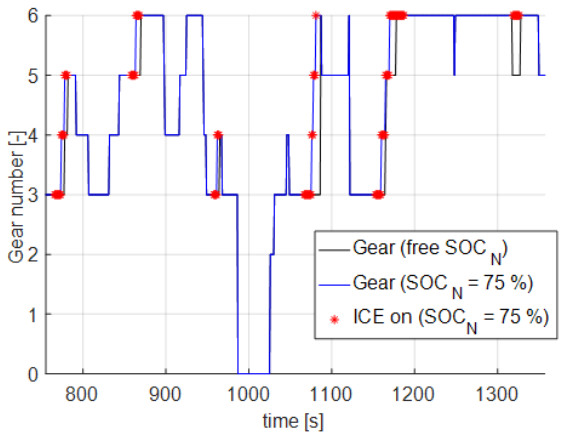

FIGURE 6. Optimal gearshift schedule variation with final SOC target.

As a consequence of the previous observations, it arises the issue of determining how the optimal solution chooses the ICE operating points. Hence, a series of simulations is undertaken in which the final SOC constraint is continuously increased. In Fig. 7, the optimal solution indicates that the most efficient operating points for the ICE are selected first and the other areas of the map with lower efficiencies are covered gradually as the use of the ICE to satisfy the final SOC constraint becomes more frequent.

Hence, the idea behind the proposed approach is that if it can be understood how the optimal solution selects the gear in EV-mode, when the ICE is needed, gear selection is simply a matter of minimizing the equivalent fuel consumption as defined in the context of the A-ECMS ([14], [40]). Based on this principle, the general structure of the algorithm is defined as shown in Fig. 8.

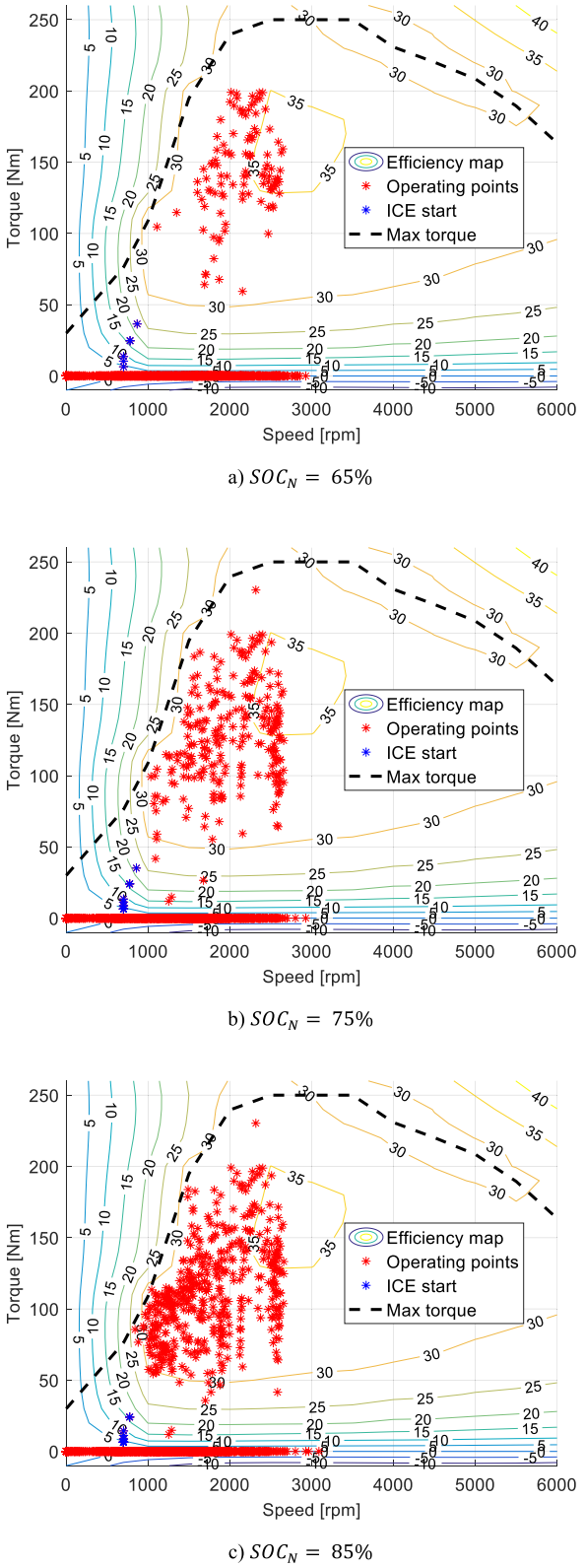

a) $SOC_N = 65\%$

b) $SOC_N = 75\%$

c) $SOC_N = 85\%$

FIGURE 7. Optimal ICE operating points variation with final SOC target: (a) $SOC_N = 65\%$; (b) $SOC_N = 75\%$; (c) $SOC_N = 85\%$.

The first task performed by the proposed EMS is to determine the gear that should be chosen for optimal EV-mode operation. This has been approached by creating

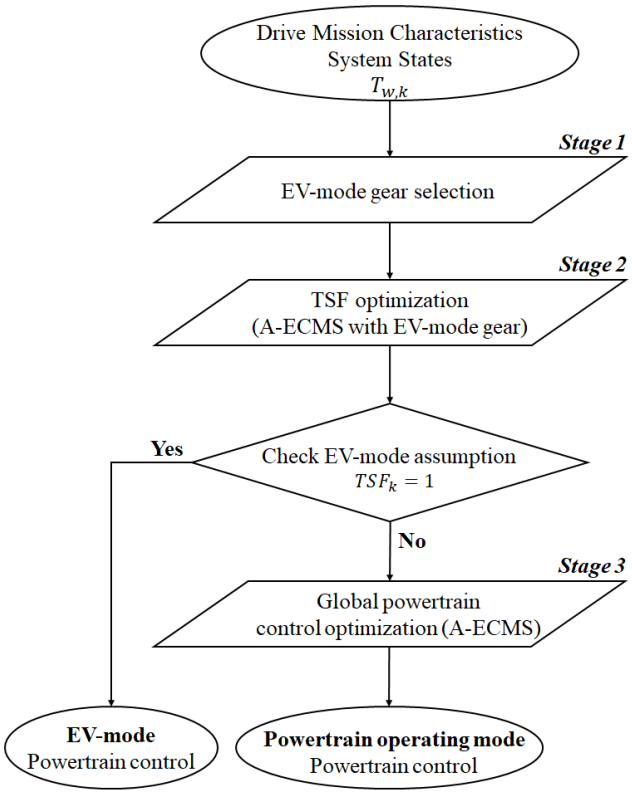

FIGURE 8. A-ECMS with rule-based gear selection general structure.

the rule-based algorithm described in section VII from the study of DP results. For the subsequent task, a specific A-ECMS formulation for the control problem is needed (see section VI) to search for the most suitable value of the TSF by imposing the gear selected at the previous stage. The idea behind this second step is to confirm the initial assumption of vehicle operation in EV-mode. If even with what should be the most suitable gear for fully electric driving, the instantaneous minimization performed by the A-ECMS still regards fuel energy use as convenient, an additional computation has to be performed. During the third stage of the process, every powertrain control variable (including the gear number) is chosen to optimize ICE operation as suggested by the observations made from Fig. 7.

It should be noted that all the inputs to the algorithm regard data coming from either the previous or current time step, thus making the proposed EMS causal. The only a-priori information needed related to the driving cycle characteristics are:

- mean speed;
- total distance to be travelled;
- duration of the driving mission.

The main algorithm outputs are:

- TSF;
- gear command;
- quick-disconnect clutch command.

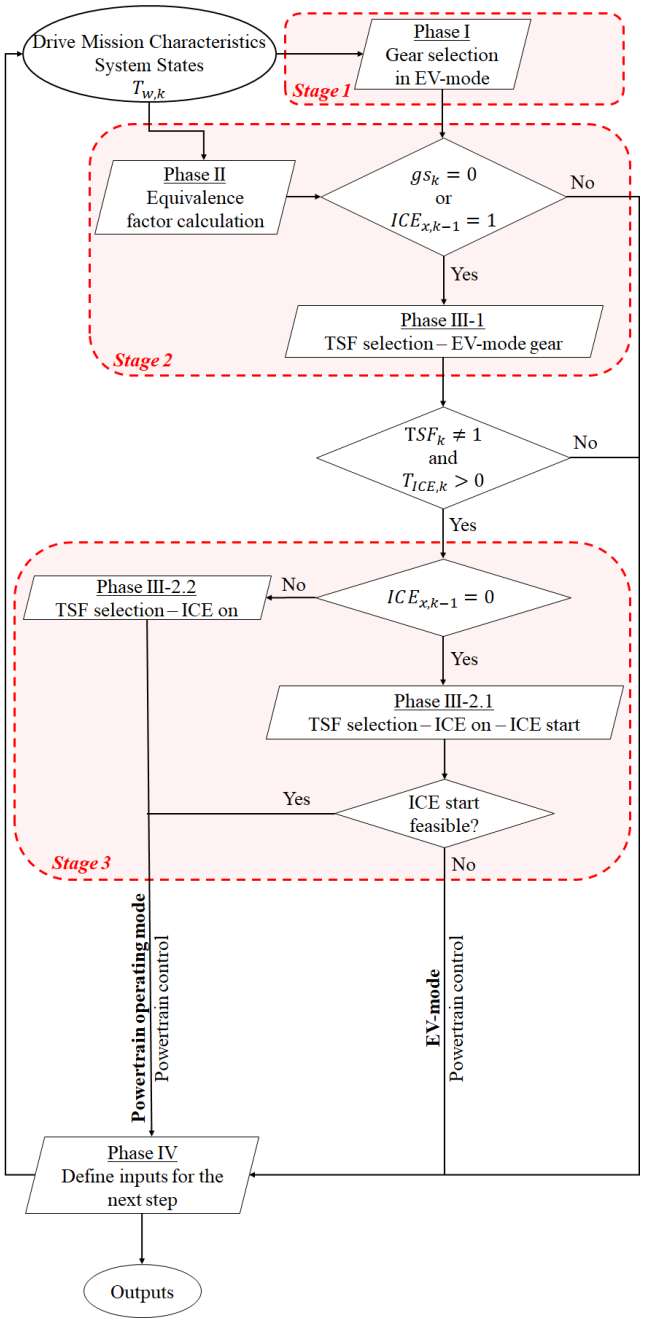

FIGURE 9. A-ECMS with rule-based gear selection flow chart.

V. ALGORITHM PHASES

The overview of the EMS provided in section IV, will be expanded in what follows, with a detailed description of the algorithm, the main assumptions and the conditions that determine the transition among different phases.

A low-level representation of the developed EMS is provided in Fig. 9.

A. PHASE I: GEAR SELECTION IN EV-MODE

As stated before, DP results are used to derive a set of rules aiming at reproducing the optimal gearshift schedule in

EV-mode. In this phase, based on the algorithm inputs and the vehicle model, the mentioned set of rules is employed to select the current gear assuming operation in EV-mode, i.e., $TSF_k = 1$ and $QD_{u,k} = 0$.

B. PHASE II: EQUIVALENCE FACTOR CALCULATION

In this phase, the A-ECMS equivalence factor is updated according to a discrete adaptation scheme based on feedback from the SOC. The reader is referred to section VI.E for more details.

C. PHASE III: TSF SELECTION

Up to this stage of the algorithm, only the gear for operation in EV-mode has been identified. However, the powertrain operating mode, or equivalently in this case the TSF, still needs to be defined. In the context of the ECMS, the TSF is selected searching for minimizing the instantaneous equivalent fuel consumption ([16]). In this phase, the TSF selection is divided in two consecutive steps:

1. based on the gear chosen in the previous phase, it is verified if the current value of the equivalence factor suggests operation in EV-mode;
2. if the computations made in step 1 indicate that it is convenient to use the ICE, the A-ECMS is employed to select the best values for the gear number and the TSF.

These calculations are undertaken in the sub-phases discussed in the following paragraphs.

It should be noted that the possibility of using the ICE is considered only when a gearshift is not suggested in the previous phase or when the quick-disconnect clutch was engaged in the preceding time step. This is because a gearshift and an ICE start event cannot occur in the same time step, to avoid increasing the complexity of the gearshift loss model used (see [30]).

D. PHASE III-1: TSF SELECTION - EV-MODE GEAR

The TSF that minimizes the instantaneous equivalent fuel consumption is identified based on the gear selected in phase I. If the selected TSF suggests operating in EV-mode, the outputs from phase I are considered. Instead, if the TSF indicates that the ICE should be employed, phase III-2 is undertaken.

E. PHASE III-2: TSF SELECTION – ICE ON

One of two possible sub-phases is undertaken according to the ICE state at the previous time instant:

- phase III-2.1: TSF –ICE start;
- phase III-2.2: TSF – ICE on.

F. PHASE III-2.1: TSF SELECTION –ICE START

This phase is active if the ICE was off in the previous step ($ICE_{x,k-1} = 0$), meaning that an ICE start process needs to be performed. Hence, the EM is responsible for supplying the power request at the wheels and a gearshift is not undertaken. It should be noted that since the vehicle does not possess a conventional starter, the EM needs to transmit power through the quick-disconnect clutch during the ICE start process (see [30]). Therefore, its speed during ICE start events must be greater than that of the ICE at all times in order to guarantee positive slip velocity while the crankshaft speed increases to match that of the EM. Based on the previous remarks, if the ICE start process is regarded as not feasible, the outputs of phase I are considered.

G. PHASE III-2.2: TORQUE SPLIT SELECTION – ICE ON

Phase III-2.2 is active when the ICE is already on, in the previous time step ($ICE_{x,k-1} = 1$). Since the ICE is employed in this phase, i.e., fuel is consumed, both the TSF and the gear number are selected to minimize the equivalent fuel consumption.

H. PHASE IV: DEFINE INPUTS FOR THE NEXT TIME STEP

Phase IV serves to define the inputs for the next iteration of the algorithm. In particular, the equivalence factor and the system states are updated. Since the strategy has been implemented in a simulation environment, the control outputs are applied to the vehicle model and the resulting system states are used as initial conditions for the next time step.

VI. A-ECMS FORMULATION

In this section, the A-ECMS formulation employed is described paying particular attention to the penalties introduced and the adaptation approach used to update the value of the equivalence factor.

A. INSTANTANEOUS MINIMIZATION

The idea at the core of the ECMS is that an equivalent fuel consumption can be associated with the use of electrical energy ([41]). Using an appropriate model of the system, the ECMS algorithm estimates the fuel and electrical energy consumption resulting for each of the possible control candidate and makes a decision aiming at locally minimizing the instantaneous equivalent fuel consumption rate which is computed as ([4], [42], [43]):

$$\dot{m}_{eq,k} = \dot{m}_{f,k} - s_k S\dot{O}C_k \tag{22}$$

where $\dot{m}_{f,k}$ is the actual fuel consumption and s_k is the equivalence factor.

In (22), the equivalence factor s_k allows converting electrical power into an equivalent amount of fuel mass flow. It should be noted that its unit is gram.

For convenience, (22) is written to define the equivalence factor as a positive quantity. In this way, the mentioned variable acts as a weighting factor in the cost function to be minimized at each iteration, i.e., the higher its value, the higher the cost of electrical energy in terms of fuel. Moreover, it should be noted that depending on the sign of the power request to the battery (which is opposite to that of the SOC rate), the equivalent fuel consumption can be either higher or lower than the actual fuel usage.

B. PENALTIES TO DISCARD INFEASIBLE WORKING CONDITIONS

The solution candidates that lead the system to infeasible working conditions are discarded by assigning a high cost, i.e., the equivalent fuel consumption is increased by a large quantity.

Infeasible working conditions are those in which the values of state variables resulting from a certain control decision lie outside of their admissible range (see section III.B). In addition, when the requests to powertrain actuators do not respect the inequality constraints defined in (21), penalties are also introduced.

C. PENALTIES TO INTRODUCE RESTRICTIONS ON THE GEAR NUMBER STATE

As explained in section II.B, integrating the models developed to estimate the energy consumption during gearshifts and ICE starts into the DP formulation for the optimal solution, yields to results with no chattering in the ICE state nor gear hunting. However, differently from the DP results, due to the instantaneous minimization approach for gear selection used in phase III-2, it was seen during the calibration stage, that it is convenient to introduce a fuel penalty (e.g. of 1 g) aiming at inducing gearshift hysteresis.

Hence, the equivalent fuel consumption is increased if an upshift is performed before a certain time has passed since the last downshift and vice versa. The time frame considered is 4 s.

D. PENALTIES TO INTRODUCE RESTRICTIONS ON THE ICE STATE

Given that in phase III of the algorithm, the TSF is selected assuming that the ICE is ready to be used, i.e., the ICE start losses are not considered, a series of fuel penalties are introduced to avoid frequent changes in the ICE state.

The first of the mentioned fuel penalties (1 g) is applied when:

- ICE is turned on before being off for less than 4 s;
- ICE is turned off before being on for less than 3 s.

Moreover, when there is a change in the ICE state, a certain increase in terms of instantaneous equivalent fuel consumption is required. A value of 0.35 g is requested to turn on the ICE. Instead, 0.2 g are considered when turning off.

Finally, as suggested by the behaviour of the optimal solution, a penalty (0.2 g) is introduced to discourage the use of the fuel energy to recharge the battery cells.

When the mentioned restrictions for changes on the ICE state are not applied, different TSFs are selected by the proposed technique with respect to those seen in the DP results. Such control decisions yield to a very intermittent ICE on/off behaviour. The driving schedule studied is again the WLTC (see Fig. 20) and the final SOC target is 75%.

On the other hand, when the fuel penalties are enforced, results improve significantly (see Fig. 10). It should be noted that "RB + A-ECMS" refers to the EMS developed which combines a rule-based gear selection in EV-mode with A-ECMS.

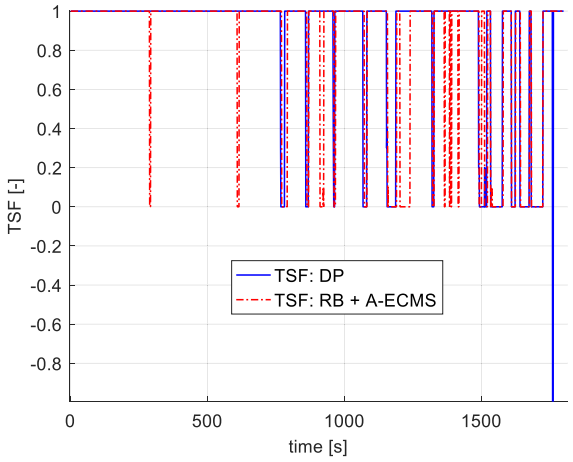

FIGURE 10. TSF: restrictions on ICE state.

E. EQUIVALENCE FACTOR ADAPTATION

The optimal equivalence factor is a function of both HEV powertrain characteristics and driving cycle features ([2]). For the EMS, a discrete adaptation scheme based on feedback from SOC is employed ([21]).

As mentioned before, for charge-depleting vehicle operation, as generally seen in PHEVs, the optimal SOC trajectory is approximately a quasi-linear decreasing function of the travelled distance ([22]–[24]).

However, when the final SOC target is set higher with respect to that encountered when looking for the global optimal solution in terms of fuel consumption (i.e., when the DP algorithm used is free to exploit all the energy available in the battery cells), it is seen for some driving cycles that a linear SOC reference defined in the time domain is more representative of the optimal solution. This can be appreciated in Fig. 11 for the WLTC where the final SOC target is raised to 75%.

Based on the previous considerations, the SOC reference used for the equivalent factor adaptation is computed as

$$SOC_{ref,k} = SOC_0 + \frac{SOC_{ref,N} - SOC_0}{NT_s} kT_s \qquad (23)$$

where SOC_0 is the initial SOC.

In the discrete adaptation law used, the equivalence factor update is performed each time a certain distance D_s is traveled ([4]):

$$s(D+D_s) = [s(D) + s(D-D_s)]/2 + K_p \left[SOC_{ref}(D) - SOC(D)\right] \qquad (24)$$

where D is the current covered distance and K_p is the proportional gain.

In (24), the two previous values of the equivalence factor are used to stabilize the output. This expression corresponds to an AutoRegressive Moving Average (ARMA) filter ([4]).

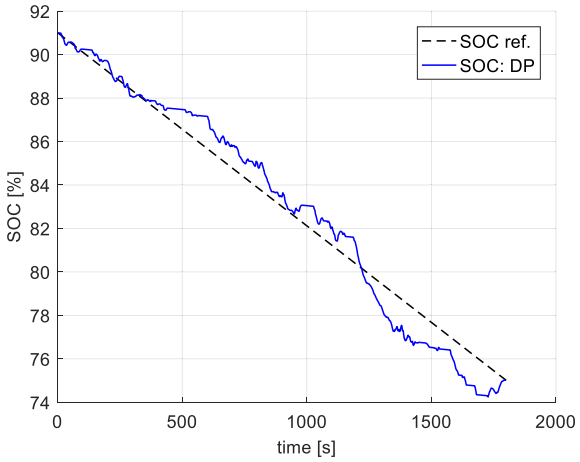

a) Time domain

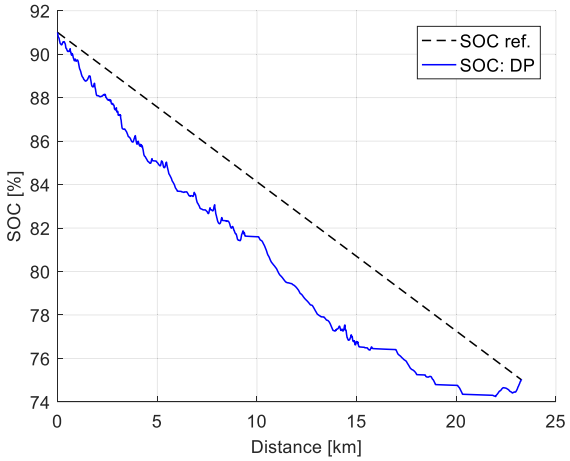

b) Distance domain

FIGURE 11. SOC reference: time domain vs. distance domain. (a) Time domain; (b) Distance domain.

Furthermore, in the adaptation law described by (24), the main SOC tracking parameters are the sampling distance D_s and the proportional gain K_p. Several simulation results for driving cycles with very different characteristics were analysed in order to properly tune the proposed strategy. These simulations showed that the developed algorithm is robust with respect to the mentioned SOC tracking parameters. Therefore, the selection of the best values for the sampling distance and the proportional gain can be made offline and the same parameters can be used regardless of the driving cycle to be followed. The values selected are: $D_s = 5$ km and $K_p = 8$ g.

It is quite obvious at this point, that selecting the most appropriate value of the initial equivalence factor is fundamental to the effectiveness of the strategy. As explained in [4], for real-time implementation, a pre-computed offline map could be used to initialize the equivalence factor based on the total distance to be travelled and the average speed of the driving mission. However, given the extensive amount of simulations needed to compute such map, this is left for future studies. In this work, the best possible values of the equivalence factor for each of the causal strategies studied are employed.

VII. RULE-BASED GEAR SELECTION IN EV-MODE

As discussed in section IV, in order to integrate a set of rules with the A-ECMS approach, such rules should be able to reproduce the optimal gearshift schedule in EV-mode. In the following, the rule extraction process is described, and the results obtained with the developed rule-based gear selection algorithm are benchmarked against the optimal solution.

A. RULE EXTRACTION PROCESS

The assumption at the basis of the process presented here is that the rules extracted from the analysis of the optimal control trajectory computed for a driving schedule which is representative of various driving conditions, should provide, after some tuning, adequate results when implemented for other speed profiles. Hence, DP simulation results for the WLTC class 3, version 3.2 ([36]), were studied with the objective of identifying certain behaviours in the optimal solution that can be turned into rules.

Charge-depleting simulations are studied in which the vehicle can follow the requested velocity trace almost entirely in EV-mode. Such analysis is focused on the points in which gearshifts are performed. The objective is to understand how the DP algorithm is choosing whether to do a downshift or an upshift and the gear number itself.

The rule extraction process followed is presented in Fig. 12.

From the diagram shown in Fig. 12, it can be appreciated that the driving cycle is examined looking for general trends in the optimal solution relating the gear number selection to the vehicle longitudinal speed. After this preliminary stage of analysis, gear selection is studied in detail by separating gearshifts into different groups:

1. single gearshifts: gearshifts without skipping gears;
2. multiple upshifts, i.e., upshifts in which gears are skipped;
3. gearshifts before braking events.

For each of these groups, gearshift decisions are studied as a function of several variables allowing to extract a specific set of rules for each of them.

Generally speaking, these rules are in the form of logical if/else conditions, based on thresholds established for a selected group of physical quantities (see Fig. 12) that allowed to properly describe the driving conditions in which the different types of gearshifts are performed. In particular, the filtered acceleration a_k and EM power rate $\dot{P}_{EM,k}$ are defined, respectively, as the derivative of the vehicle longitudinal speed v_k and EM power $P_{EM,k}$, computed every two time steps instead of considering consecutive samples. This is a simple way to remove some disturbances in the studied variable trends. Moreover, the EM power loss $P_{EM,dis,k}$ is computed as the difference between the actual EM power

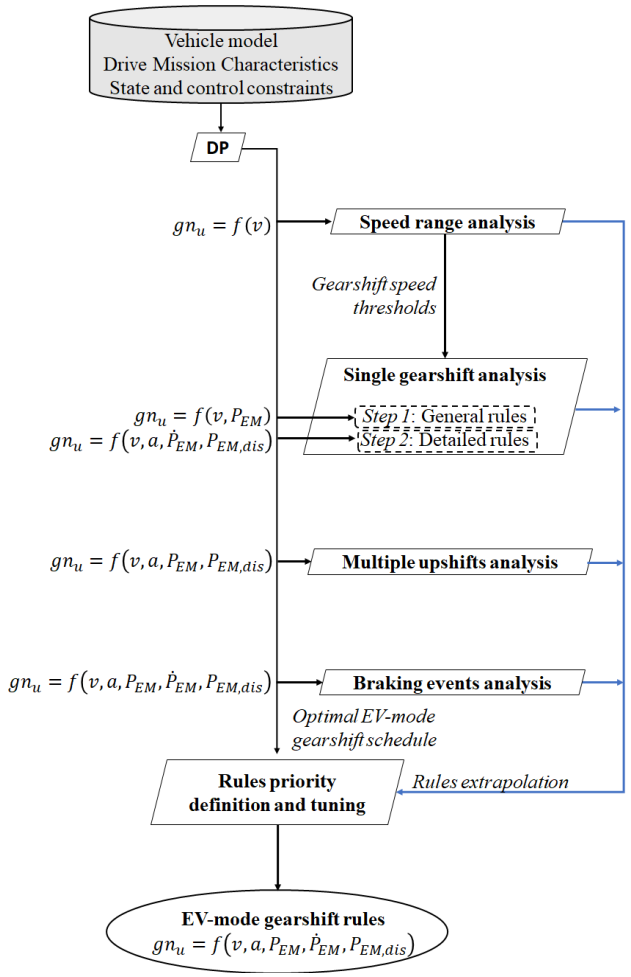

FIGURE 12. EV-mode gear selection rules extraction process.

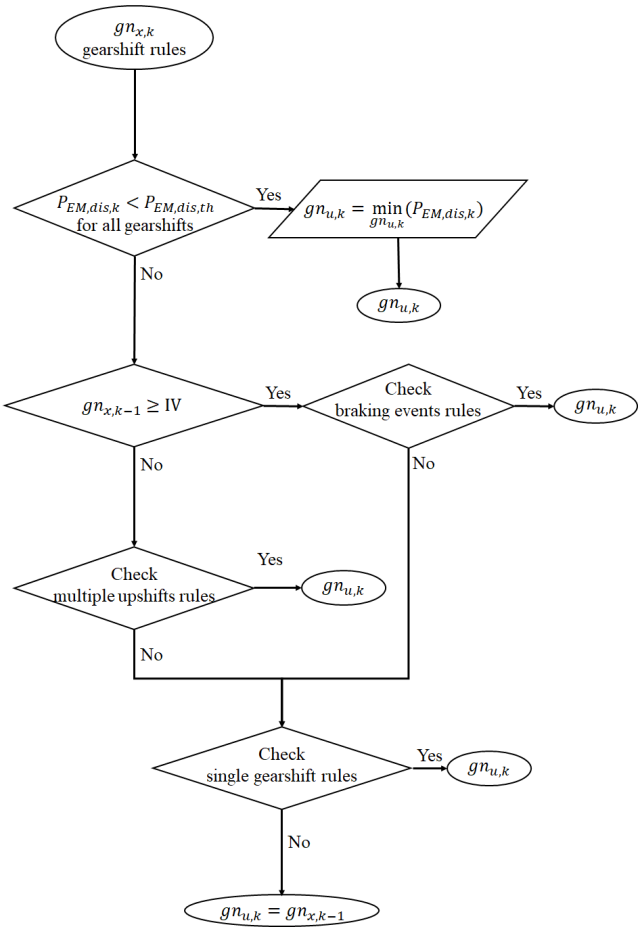

FIGURE 13. EV-mode gear selection flowchart.

request (considering the gearshift losses) and the power consumption of the no gearshift case. Hence, negatives values of this quantity imply energy savings as a consequence of the gearshift process.

While for the single gearshifts, the decision to perform each manoeuvre is driven by several factors, energy consumption is the main variable behind the selection of the other two types of shifts.

For example, it was observed that, when the vehicle speed increases, multiple upshifts are performed if the EM power request is very close (within 300 W) to that of the single gearshift.

On the other hand, the analysis of all the gearshift manoeuvres performed revealed that only a small amount involved an EM power loss higher than 20% with respect to the power consumption of the no gearshift case. If the points in which such power dissipation is lower than 350 W are excluded, almost all the remaining gearshifts correspond to downshifts that occurred right before a braking event. It should be noted that choosing the appropriate gear when decelerating, is crucial for any well-designed EMS since it allows to maximize the energy regenerated with the EM that otherwise will be dissipated by the mechanical brakes.

Since the mentioned sets of rules are extracted independently, the final phase of the overall process consists on establishing a hierarchical structure and to properly tune the defined thresholds. To achieve this, an iterative procedure is performed in which the effectiveness of the gear selection algorithm after each modification is tested comparing the obtained gearshift schedule with the optimal solution.

In appendix III, the analysis of the optimal solution during the rule extraction process is illustrated for each of the defined gearshift groups.

B. RULE-BASED GEAR SELECTION ALGORITHM

From the rule extraction process reviewed in section VII.A, an algorithm for gear selection in EV-mode is designed (see Fig. 13).

As it can be appreciated form the diagram in Fig. 13, the first step in the EV-mode gear selection process is to verify the EM power loss for all possible shifts. If values lower than a certain threshold are found (in this case -1kW is chosen after some tuning) the gear selected will be the one yielding the lowest energy loss.

On the other hand, if energy savings with respect to the no gearshift case are not sufficient, two possible checks are performed based on the engaged gear at the previous time

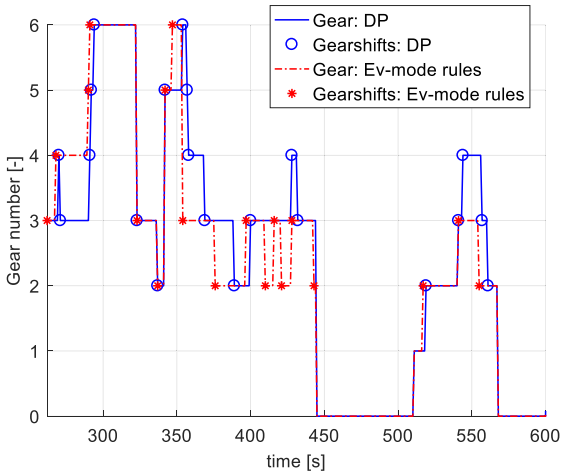

FIGURE 14. EV-mode: gearshift rules benchmarking.

step. For high gears (4^{th} to 6^{th}), the conditions established for gearshifts before braking events are verified, otherwise, the rules for multiple upshifts are to be considered.

It should be noted that the set of conditions/rules designed for single gearshift events are only verified at the end of the process. It was found during the priority definition and tuning phase of the rule extraction procedure (see Fig. 12) that this is necessary in order to properly replicate the optimal gear schedule and SOC profile in EV-mode. As mentioned in the previous paragraph, the rules for multiple upshifts and for gearshifts before braking events are mostly driven by energy consumption concerns. This implies that in the DP results, gear selection is controlled to optimize the use of electrical energy, thus avoiding fuel-consumption.

Fig. 14 shows the gearshift schedule obtained after implementing the EV-mode gearshift rules for the same velocity profile analysed in section VII.A. In general, the optimal gear number state trajectory is reproduced. However, there are also several instances in which different decisions are taken. Since the rules do not rely on the knowledge of the future driving conditions, when certain speed and power trends are present in the driving cycle, the rule-based approach tends to anticipate the decisions made with DP.

Even though some different gearshift decisions are visible in Fig. 14, the optimal SOC profile is well reproduced. The similar SOC trend (final SOC difference lower than 0.5%) is obtained due to the ability of the rule-based approach to recognize relevant speed and power trends in the driving cycle. In particular, it is worth underlining that the gear number selected before important braking events coincides with that of the optimal solution in most cases.

Table 2 presents the gear selected by the rule-based approach for some of the braking events with the highest power available for regeneration (highest, in absolute terms, mechanical power request to EM P_{reg}): by implementing the EV-mode gearshift rules, a similar gear with respect to that seen in the optimal solution is chosen.

TABLE 2. Braking events: WLTC.

t [s]	757	795	902	1125	1729
P_{reg} [kW]	-28.57	-38.17	-31.23	-43.77	-31.96
gn: DP	3	4	4	3	6
gn: RB	3	4	4	4	5

VIII. SIMULATION RESULTS

In this section, the optimal solution to the energy management problem obtained with DP is used to benchmark the results provided by the developed EMS (referred to as RB + A-ECMS) and those of the A-ECMS.

For the A-ECMS implementation, the same powertrain model, penalties and equivalence factor adaptation scheme employed for the EMS described in the previous paragraphs, are considered. It should be noted that according to the A-ECMS approach, at each iteration, the instantaneous equivalent fuel consumption is minimized by choosing both the TSF and the most appropriate gear. The strategy was tuned to maximize its performance, thus allowing a fair comparison with the alternative control technique proposed in this work.

To undertake this benchmark, suitable metrics should be defined. Consider for example a case in which two different EMSs yield the same fuel consumption but with different final SOC. It is quite obvious that in terms of energy usage, the one with the highest SOC outperforms the other. This simple example is meant to illustrate that in order to make a fair comparison of the energy consumption for different strategies, it is necessary to account for the energy left in the battery. Hence, similarly to [19] and [44], a total equivalent fuel mass is defined considering the fuel savings obtained by not providing the net amount of energy supplied by the battery through the thermal path, i.e.:

$$m_{eq,t} = m_{f,t} + \frac{E_{b,t}}{\bar{\eta}_{ICE} LHV} \tag{25}$$

where $E_{b,t}$ is the total energy provided by the battery during a driving mission, LHV is the fuel lower heating value and $\bar{\eta}_{ICE}$ is the mean efficiency of the ICE during vehicle operation.

The effectiveness of real-time implementable control strategies will be evaluated by using as a parameter the difference between the total equivalent fuel mass of the causal EMS and that of the optimal solution, i.e.:

$$\Delta m_{eq,t} = \frac{m_{eq,t} - m^*_{eq,t}}{m^*_{eq,t}} 100 \tag{26}$$

where $m^*_{eq,t}$ is the optimal total equivalent fuel mass.

In addition, the percentage difference in the total fuel consumption will also be considered, defined as:

$$\Delta m_{f,t} = \frac{m_{f,t} - m^*_{f,t}}{m^*_{f,t}} 100 \tag{27}$$

where $m^*_{f,t}$ is the optimal total fuel consumption.

Having defined the necessary metrics, simulation results for four driving cycles are discussed to illustrate the controller capabilities and limitations. The first of the driving schedules considered is the WLTC class 3, version 3.2, used for the development of the strategy. As explained in section VII, this cycle was analysed to extract the set of rules employed for gear selection in EV-mode. Moreover, the US06 driving cycle (see Fig. 21), which is representative of aggressive highway driving conditions in the USA ([44]), is also considered. The cycle is characterized by portions with rapid speed fluctuations and high acceleration ([45]). The FUDS (see Fig. 22) allowed to test the EMS in an urban route with frequent stops ([45]). Finally, a driving mission that blends a series of EPA (Environmental Protection Agency) test cycles, which makes it representative of real-world driving conditions, is also used to validate the proposed strategy (see Fig. 23). It should be noted that by analysing these driving cycles, the effectiveness of the algorithm can be assessed for different working conditions ranging from typical urban driving behaviour to aggressive highway driving. The main characteristics of the mentioned speed profiles are summarized in Appendix II.

The simulation results were computed within Matlab/Simulink environment. The main parameters characterizing the simulation setup for each of the previously mentioned driving cycles are:

- time step: 1s;
- initial SOC: 91%;
- final SOC target: 75%;
- minimum allowed SOC at mission end: 74%;
- number of cycle repetitions: set to allow testing different driving profiles with a similar total distance (see Tables 3 and 4).

Fig. 15 illustrates the results of the RB + A-ECMS for the WLTC. The SOC trajectory is very close to the optimal one through the entire cycle. It can also be appreciated that both the total fuel consumption and the final SOC are similar to those obtained with DP. The latter is also valid for the results of the A-ECMS.

Fig. 16 shows the EM operating points for both the DP solution and the RB + A-ECMS approach. It should be noticed that the EM continuous torque limit is breached more times in the online implementable approach than in the DP results. On the other hand, by comparing the ICE operating points (see Fig. 17), it can be stated that in both cases the ICE working conditions are selected to operate in the map region related to lower fuel consumption rates and higher efficiencies.

For the blended cycle, Fig. 18 shows that the optimal SOC trajectory is consistently different from the given reference. Moreover, in the RB + A-ECMS results, the SOC is kept closer to the reference provided while with the A-ECMS the energy storage system operates at lower values. This clearly illustrates a limitation of the equivalence factor adaptation schemes based on feedback from SOC: a technique to generate reference profiles for the SOC which are representative

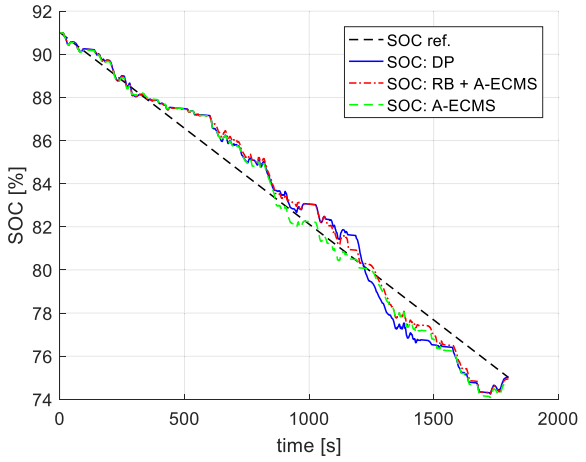

a) SOC

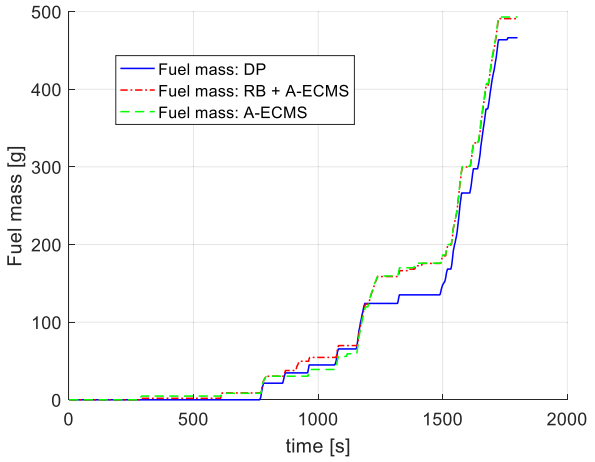

b) Fuel consumption

FIGURE 15. Benchmarking results: WLTC. (a) SOC; (b) Fuel consumption.

of the optimal solution regardless of the driving cycle is not available.

Tables 3 and 4 summarize the most relevant parameters for the benchmarking of the RB + A-ECMS and A-ECMS approaches. It can be concluded that, in terms of the total equivalent fuel consumption, the RB + A-ECMS approach does not only yield results that are close to the optimal solution (within 8%) but also outperforms those of the A-ECMS. The mentioned EMS also provides better results than the A-ECMS in terms of the actual fuel consumption.

As expected, the controller performs better for the cycle used during its development. However, it proves to be a valid alternative to other well-known techniques as the A-ECMS even for velocity traces which are fundamentally different from that of the WLTC.

The total number of gearshifts is reported in Table 5 for all the driving schedules and EMSs studied. The RB + A-ECMS approach tends to result in more gearshifts than those performed in the optimal solution while the A-ECMS does the

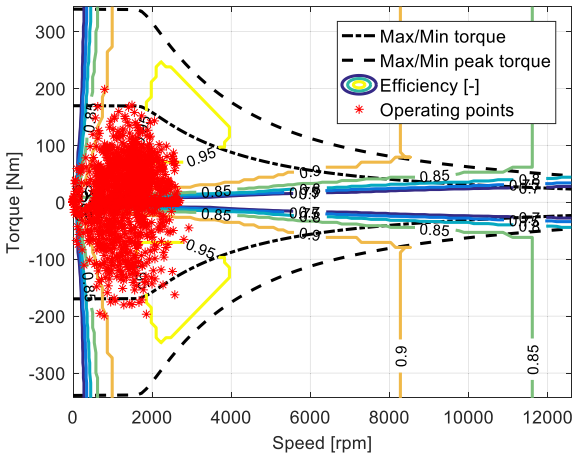

a) DP

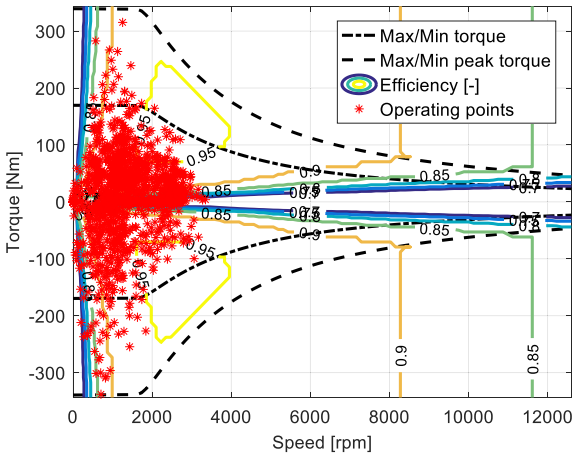

b) RB + A-ECMS

FIGURE 16. EM operating points: WLTC. (a) DP; (b) RB + A-ECMS.

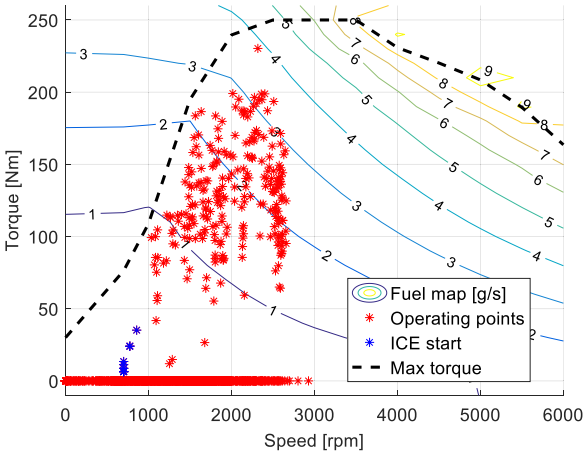

a) DP

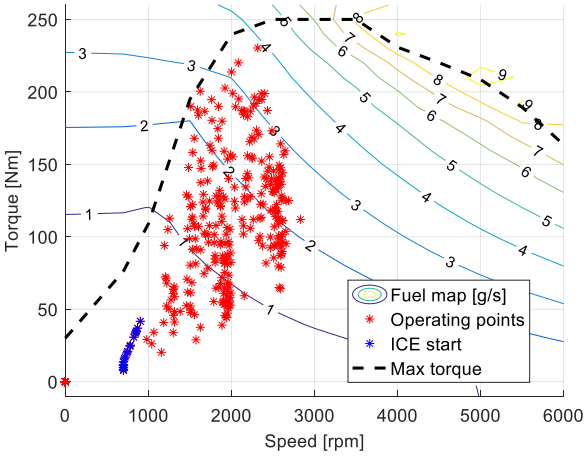

b) RB + A-ECMS

FIGURE 17. ICE operating points: WLTC. (a) DP; (b) RB + A-ECMS.

TABLE 3. Benchmarking results: RB + A-ECMS.

Parameter	WLTC	FUDS (2 rep.)	US06 (2 rep.)	Blended cycle
$\Delta m_{eq,t}$ [%]	3.739	7.565	6.035	2.642
$\Delta m_{f,t}$ [%]	5.266	11.471	9.560	13.356
SOC_N [%]	74.937	74.857	75.388	76.145

TABLE 4. Benchmarking results: A-ECMS.

Parameter	WLTC	FUDS (2 rep.)	US06 (2 rep.)	Blended cycle
$\Delta m_{eq,t}$ [%]	4.444	10.214	7.383	7.948
$\Delta m_{f,t}$ [%]	5.720	15.889	12.589	20.661
SOC_N [%]	74.790	74.510	75.996	75.789

TABLE 5. Number of gearshifts.

EMS	WLTC	FUDS (2 rep.)	US06 (2 rep.)	Blended cycle
DP	99	166	44	68
RB + A-ECMS	127	175	96	73
A-ECMS	78	156	54	44

opposite. For the blended cycle, Fig. 19 shows that the higher number of gearshifts seen for the RB + A-ECMS technique enable this strategy to better reproduce the optimal gearshift schedule when compared to the results of the A-ECMS.

Furthermore, data in Tables 3 and 4 allows appreciating that the RB + A-ECMS approach yields a higher final SOC for WLTC, FUDS and the blended cycle with respect to A-ECMS. From the analysis of the simulation results, it was inferred that this could be related to a more efficient regeneration of electrical energy during braking events.

In particular, the FUDS, with a velocity profile characterized by frequent stops, presents several opportunities for energy regeneration. Table 6, analogous to Table 2, presents

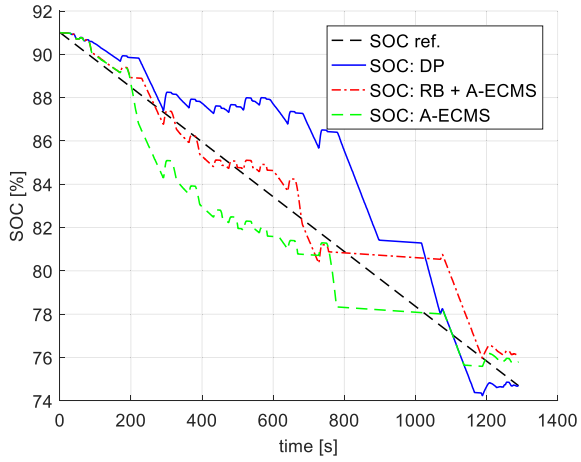

a) SOC

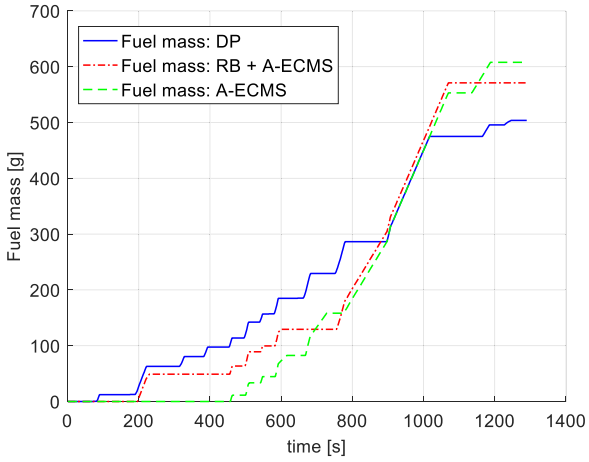

b) Fuel consumption

FIGURE 18. SOC and fuel consumption: blended cycle. (a) SOC; (b) Fuel consumption.

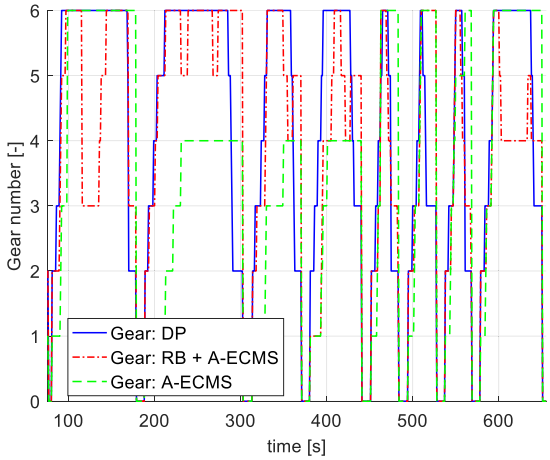

FIGURE 19. Gearshift schedule: blended cycle (zoom).

the gear selected by the studied EMSs for the braking events presenting the highest power available for regeneration at the EM shaft. As seen for the WLTC, in general,

TABLE 6. Braking events: FUDS.

t [s]	104	409	601	1293	1463
P_{reg} [kW]	-25.79	-22.04	-22.67	-24.35	-25.79
gn: DP	3	3	3	3	3
gn: RB + A-ECMS	3	6	4	3	3
gn: A-ECMS	6	6	5	3	6

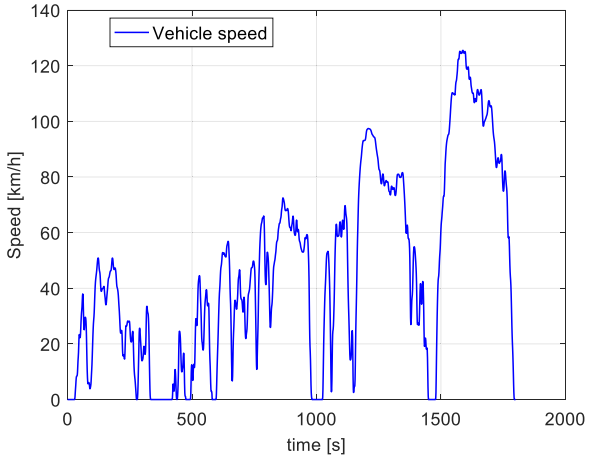

a) Speed

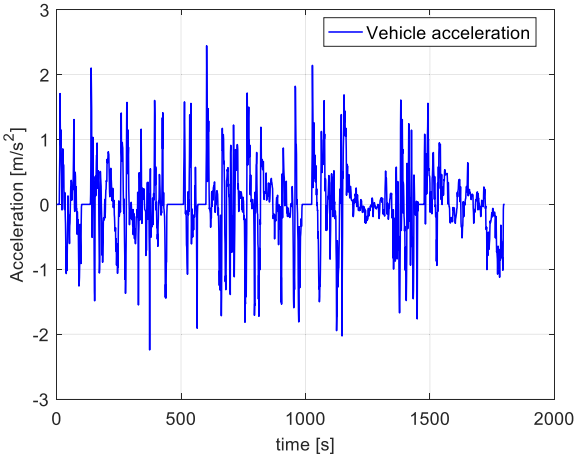

b) Acceleration

FIGURE 20. WLTC class 3, version 3.2. (a) Speed; (b) Acceleration.

the EV-mode gearshift rules, enable the RB + A-ECMS approach to enforce operation in a similar gear with respect to that chosen by DP. Instead, the instantaneous minimization approach used in the A-ECMS, tends to choose higher gears.

In addition, as shown in Table 7, the tendency of the proposed EMS to select the most appropriate gear before important braking events is also evident for the blended cycle. It should be noted that with respect to the FUDS, this driving mission presents fewer opportunities for energy regeneration that are characterized by higher power values. Furthermore,

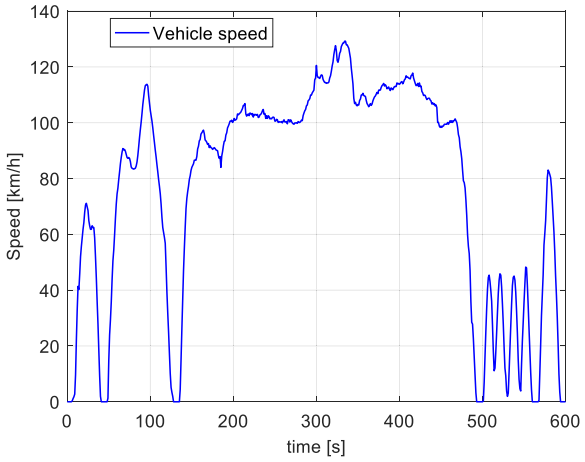

a) Speed

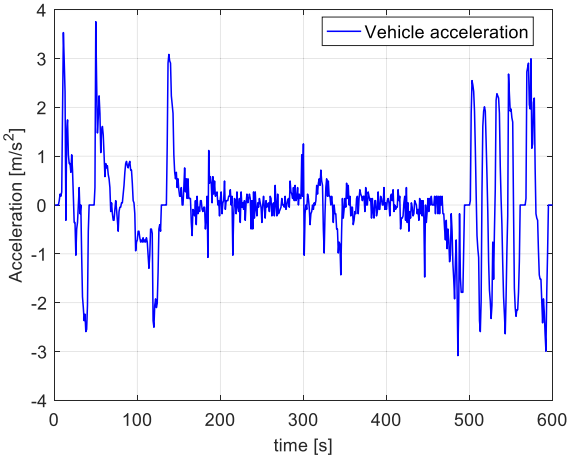

b) Acceleration

FIGURE 21. US06. (a) Speed; (b) Acceleration.

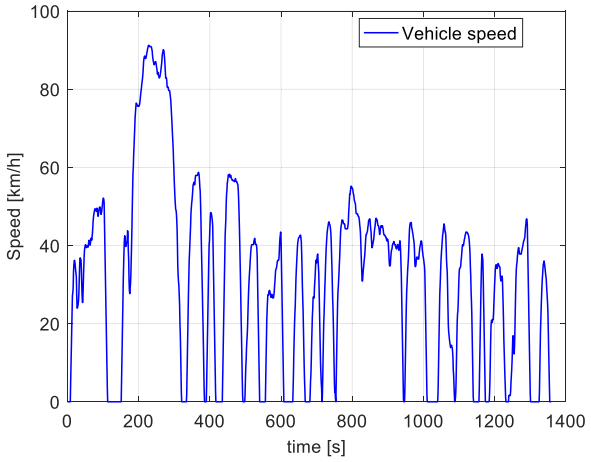

a) Speed

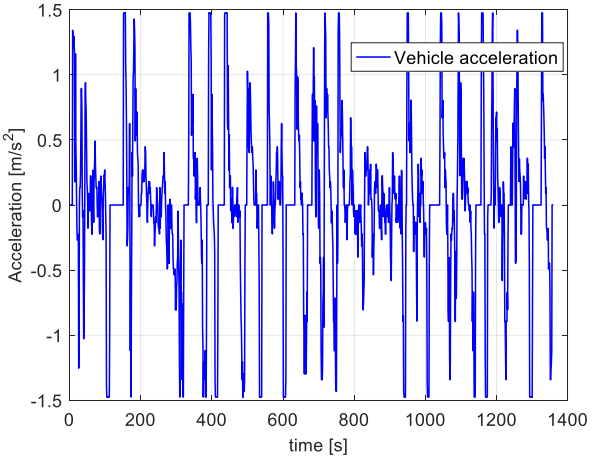

b) Acceleration

FIGURE 22. FUDS. (a) Speed; (b) Acceleration.

TABLE 7. Braking events: blended cycle.

t [s]	295	366	519	643	731
P_{reg} [kW]	-68.52	-46.52	-52.51	-55.08	-73.21
gn: DP	6	6	5	3	5
gn: RB + A-ECMS	5	6	4	3	4
gn: A-ECMS	4	4	6	6	6

it should be noted that the propensity of the A-ECMS for choosing higher gears is more in agreement with the optimal solution for this cycle than it was for the FUDS.

IX. CONCLUSION

In this work, a causal EMS has been designed. The idea behind the proposed approach is that if it can be understood how the optimal solution selects the gear in EV-mode, when the ICE is needed, gear selection is then simply a matter of minimizing the equivalent fuel consumption as defined in the context of the ECMS. This is inferred from a series of observations made based on the optimal solution behaviour. Hence, for the development of the strategy, DP results are used to derive a set of rules aiming at reproducing the optimal gearshift schedule in EV-mode while the A-ECMS was selected to decide the powertrain operating mode (through the TSF) and the current gear if power from the ICE is needed.

As for the DP formulation presented in [30], one fundamental aspect that differentiates the real-time implementable EMSs developed here from those published in previous works, is the modelling of the energy consumption during gearshifts and ICE starts. Appropiate modelling of the power losses during these transient events together with the fuel penalties introduced allowed the controller to yield results in which there is no gear hunting behaviour or chattering in the ICE state. It should be noted that this is a rather common problem for control techniques based on an instantaneous minimization.

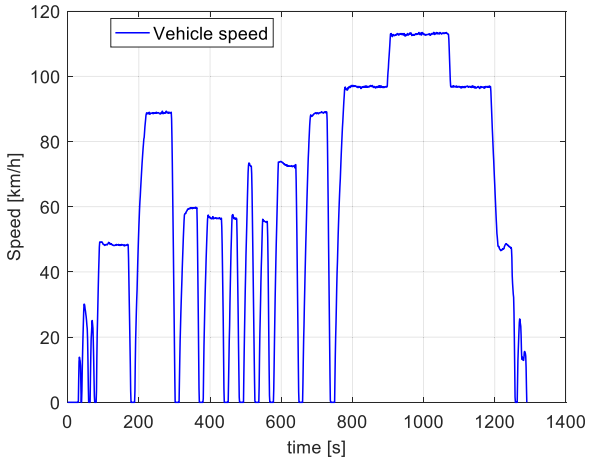

a) Speed

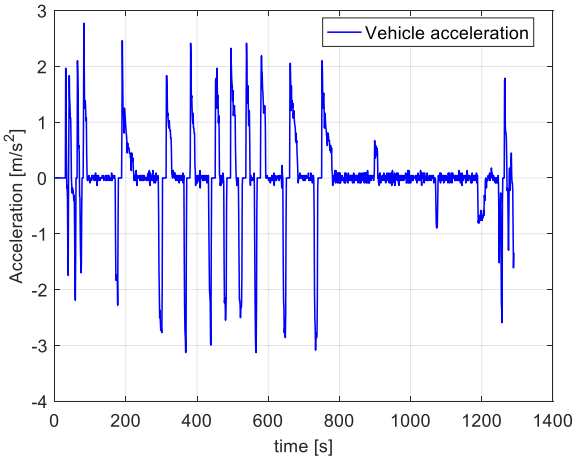

b) Acceleration

FIGURE 23. Blended cycle. (a) Speed; (b) Acceleration.

In the causal strategies utilised in this work, a discrete adaptation scheme based on feedback from SOC was employed. By analysing the optimal solution, it was concluded that, depending on the driving cycle characteristics and final SOC target, the linear SOC reference that is more in agreement with the DP results could be defined in either the time or the distance domain. This clearly illustrates a limitation of the adaptation schemes from the literature: no technique to generate reference profiles for the SOC which are representative of the optimal solution regardless of the driving schedule to be followed is available.

Nevertheless, simulation results show that, in terms of total equivalent fuel consumption, the RB + A-ECMS approach does not only yield results that are close to the optimal solution but also outperforms those of the A-ECMS. This EMS also provides better results than the A-ECMS in terms of actual fuel consumption. In addition, both causal strategies proved to be robust with respect to SOC tracking parameters.

When analysing the behaviour of the solutions, it is observed that, in general, the implementation of the RB + A-ECMS approach foresees a larger number of gearshifts than those performed in the optimal solution, while the A-ECMS does the opposite. Thanks to the ability of the designed rules to recognize relevant speed and power trends in the driving cycle, the gear number selected before high power braking events is similar to the optimal one in most cases. Finally, it should be noted that choosing the appropriate gear maximizes the energy regenerated with the EM.

APPENDIX I

ABBREVIATIONS

A-ECMS	Adaptive Equivalent Consumption Minimization Strategy
ARMA	AutoRegressive Moving Average
DCT	Dual-Clutch Transmission
DCU	Dual-Clutch Unit
DP	Dynamic Programming
ECMS	Equivalent Consumption Minimization Strategy
EM	Electric Machine
EMS	Energy Management Strategy
EPA	Environmental Protection Agency
EV	Electric Vehicle
FUDS	Federal Urban Driving Schedule
HEV	Hybrid Electric Vehicle
ICE	Internal Combustion Engine
LHV	Lower Heating Value
PHEV	Plug-in Hybrid Electric Vehicle
PMP	Pontryagin's Minimum Principle
RB	Rule-Based
SOC	State Of Charge
TSF	Torque Split Factor
WLTC	World-wide harmonized Light duty Test Cycle

NOTATION

a	Vehicle longitudinal acceleration
D	Distance
es	ICE start status
E	Energy
f	Generic function
gn	Gear number
gs	Gearshift status
I	Electric current
J	Mass moment of inertia
k	Discrete step
K	Generic gain
L	Cost function
m	Mass
$\dot{m}$	Fuel consumption
P	Power
Q	Electric capacity
QD	Quick-disconnect clutch
s	Equivalence factor
t	Time
T	Torque

u	Control variable
U	Control domain
v	Vehicle longitudinal speed
x	Discrete state variable
X	State domain
Δm	Mass difference
$\Delta\omega$	Angular speed difference
Δx	Range for state variables
η	Efficiency
T	Time length
T_s	Computation step duration
Ψ	Performance index
τ	Transmission ratio
ω	Angular speed

SUBSCRIPTS AND SUPERSCRIPTS

0	Initial condition
b	Battery element
c	Clutch
cds	ICE cold start
dis	Dissipative element
eq	Equivalent element
k	Time step counter (integer)
f	Final element (when used for indexing)
f	Fuel
fd	Final drive
j	Generic index
lim	Limit related element
$loss$	Power loss
max	Maximum value
min	Minimum value
nom	Nominal element
N	final time step counter
p	Proportional element
ref	Reference
reg	Regeneration
s	Sampling related element
t	Total
tot	Total
tgt	Target
u	Control
v	Vehicle
w	Wheel
x	State
$*$	Optimality
$\dot{}$	Time derivative

APPENDIX II

This appendix shows the speed and acceleration profiles of the driving cycles analysed in this work.

APPENDIX III

This appendix illustrates some of the observations drawn from the optimal solution regarding gear selection in EV-mode.

TABLE 8. Driving cycles.

Parameter	WLTC	FUDS	US06	Blended cycle
Duration [s]	1800	1372	596	1290
Distance [km]	23.27	12.07	12.8	22.72
Average speed [km/h]	46.5	31.5	77.9	63.4
Maximum speed [km/h]	131.3	91.2	129.2	113.4

TABLE 9. Speed ranges for gear selectio.

New gear number	Speed range [m/s]
2	< 6
3	4 to 17
4	6 to 20
5 and 6	> 6

A. SPEED RANGE ANALYSIS

Table 9 summarizes the results obtained from the examination of the vehicle speed and the gear engaged after each gearshift.

It should be noted that such speed ranges are not strictly respected for all gearshift events but rather represent a general trend observed in the simulation results.

B. SINGLE GEARSHIFTS ANALYSIS

Fig. 24 and Fig. 25 show the downshifts and upshifts performed in the EM power and vehicle speed plane.

From the data presented in Fig. 24, the following observations can be made about the downshift manoeuvres:

- most gearshifts are performed for EM power requests lower than 7 kW;
- no gearshifts are performed for EM power requests lower than 450 W;
- no downshifts to 1st gear are performed in EV-mode.

Instead, for the upshift manoeuvres (see Fig. 25):

- most gearshifts are performed for EM power requests lower than 20 kW;
- no gearshifts are performed for EM power requests lower than 250 W;

After this first set of observations, the optimal gearshift schedule was studied in detail. To illustrate this process, the characteristics of the gearshift points found in a particular driving cycle section are summarized in Table 10.

The aforementioned observations can be summarized as:

- From gearshifts at 291 and 292 s: if the vehicle speed is increasing and the EM power request decreases, upshifts are performed;
- From the gearshift at 294 s: 5th to 6th upshifts are performed for speeds lower than 20 m/s and negative EM power loss;

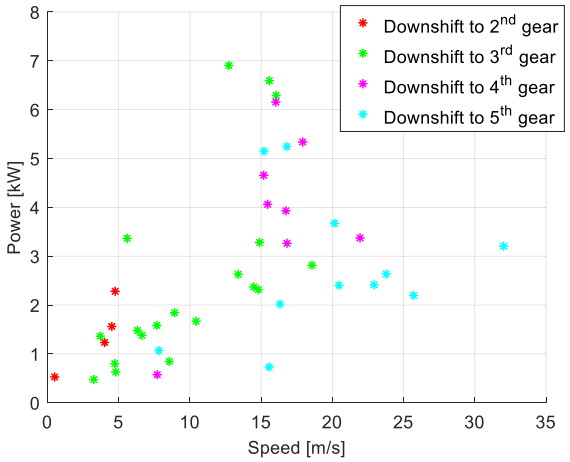

FIGURE 24. EV-mode: EM power and vehicle speed plane (downshifts).

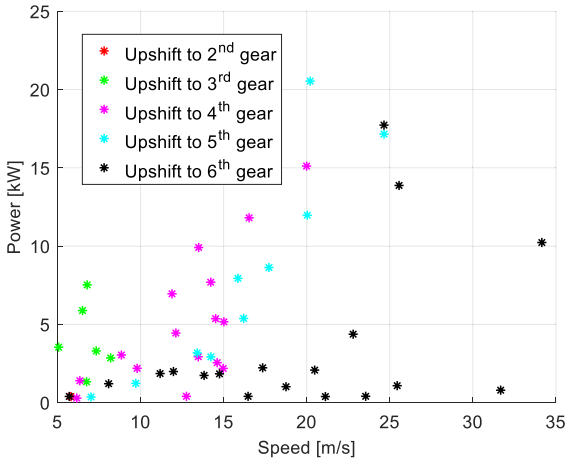

FIGURE 25. EV-mode: EM power and vehicle speed plane (upshifts).

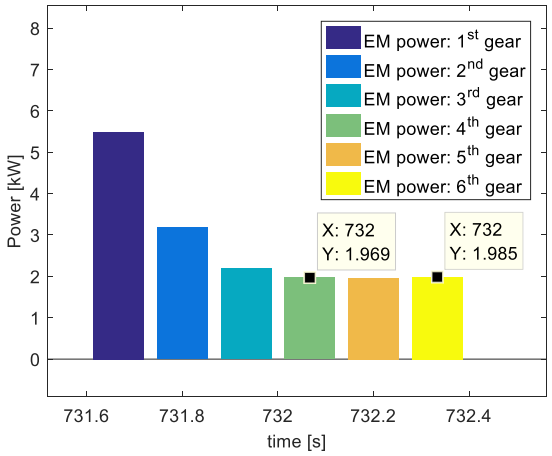

FIGURE 26. EV-mode: EM power request for all gears (732 s).

- From gearshift at 337 s: with speeds lower than 5 m/s with increasing power request, downshifts to 2nd gear are performed;
- From gearshifts at 357 and 358 s: if the vehicle speed decreases and the EM power request also diminishes, a downshift is undertaken.

TABLE 10. Gearshift points data.

t [s]	Gearshift	v [m/s]	a [m/s^2]	$\dot{P}_{EM}$ [kW/s]	$P_{EM,dis}$ [W]
291	III-IV	14.22	0.37	-9.817	555
292	IV-V	14.23	0.09	-4.182	67
294	V-VI	13.82	-0.20	-0.539	-39
337	III-II	4.00	-0.15	0.667	237
357	VI-V	7.81	-0.09	-0.044	106
358	V-IV	7.71	-0.10	-0.314	190

By looking at the same variables studied here in other portions of the driving cycle, the complete set of rules for single gearshifts was derived.

C. MULTIPLE UPSHIFTS ANALYSIS

It was observed that, when the vehicle speed increases, multiple upshifts are performed if the EM power request is very close (within 300 W) to that of the single gearshift. An example of this is the 3rd to 6th upshift for which the power consumption is reported in Fig. 26.

D. BRAKING EVENTS ANALYSIS

After reviewing each of the gearshifts undertaken before braking events, the following trends were observed in the optimal solution:

- for 6th to 3rd gearshifts:
  - EM power rate is lower than -1 kW/s;
  - EM power loss is lower than 1.1 kW;
- for 5th to 4th gearshifts:
  - vehicle speed is higher than 17 m/s;
  - EM power loss is lower than 600 W;
- for 4th to 3rd gearshifts:
  - vehicle speed is higher than 14 m/s;
  - EM power rate is lower than -1.3 kW/s;
  - EM power loss is lower than 1.1 kW.

REFERENCES

[1] T. J. Böhme and B. Frank, *Hybrid Systems, Optimal Control and Hybrid Vehicles?: Theory, Methods and Applications*, 1st ed. Cham, Switzerland: Springer, 2017.
[2] S. Onori, L. Serrao, and G. Rizzoni, *Hybrid Electric Vehicles: Energy Management Strategies*, 1st ed. London, U.K.: Springer-Verlag, 2016.
[3] N. Kim, S. Cha, and H. Peng, "Optimal control of hybrid electric vehicles based on Pontryagin's minimum principle," *IEEE Trans. Control Syst. Technol.*, vol. 19, no. 5, pp. 1279–1287, Sep. 2011.
[4] S. Onori and L. Tribioli, "Adaptive Pontryagin's minimum principle supervisory controller design for the plug-in hybrid GM chevrolet volt," *Appl. Energy*, vol. 147, pp. 224–234, Jun. 2015.
[5] D. Bertsekas, *Dynamic Programming and Optimal Control*. Belmont, MA, USA: Athena Scientific, 1995.
[6] C.-C. Lin, H. Peng, J. W. Grizzle, and J.-M. Kang, "Power management strategy for a parallel hybrid electric truck," *IEEE Trans. Control Syst. Technol.*, vol. 11, no. 6, pp. 839–849, Nov. 2003.
[7] V. D. Ngo, J. A. Colin Navarrete, T. Hofman, M. Steinbuch, and A. Serrarens, "Optimal gear shift strategies for fuel economy and driveability," *Proc. Inst. Mech. Eng. D, J. Automobile Eng.*, vol. 227, no. 10, pp. 1398–1413, Oct. 2013.
[8] L. Serrao, S. Onori, and G. Rizzoni, "A comparative analysis of energy management strategies for hybrid electric vehicles," *J. Dyn. Syst., Meas., Control*, vol. 133, no. 3, p. 31012, May 2011.

[9] C.-C. Lin, Z. Filipi, L. Louca, H. Peng, D. Assanis, and J. Stein, "Modelling and control of a medium-duty hybrid electric truck," *Int. J. Heavy Veh. Syst.*, vol. 11, nos. 3–4, pp. 349–371, 2004.

[10] D. Bianchi, L. Rolando, L. Serrao, S. Onori, G. Rizzoni, N. Al-Khayat, T.-M. Hsieh, and P. Kang, "A rule-based strategy for a series/parallel hybrid electric vehicle: An approach based on dynamic programming," in *Proc. ASME Dyn. Syst. Control Conf.*, Jan. 2010, pp. 507–514.

[11] D. Bianchi, L. Rolando, L. Serrao, S. Onori, G. Rizzoni, N. Al-Khayat, T.-M. Hsieh, and P. Kang, "Layered control strategies for hybrid electric vehicles based on optimal control," *Int. J. Electr. Hybrid Veh.*, vol. 3, no. 2, pp. 191–217, 2011.

[12] D. Kum, H. Peng, and N. K. Bucknor, "Optimal control of plug-in HEVs for fuel economy under various travel distances," *IFAC Proc. Volumes*, vol. 43, no. 7, pp. 258–263, Jul. 2010.

[13] L. Serrao, S. Onori, and G. Rizzoni, "A comparative analysis of energy management strategies for hybrid electric vehicles," *J. Dyn. Syst., Meas., Control*, vol. 133, no. 3, 2011.

[14] G. Paganelli, "Conception et commande d'une chaîne de traction pour véhicule hybride paralléle thermique et électrique," Ph.D. dissertation, Univ. Valenciennes, Famars, France, 1999.

[15] A. Sciarretta, M. Back, and L. Guzzella, "Optimal control of parallel hybrid electric vehicles," *IEEE Trans. Control Syst. Technol.*, vol. 12, no. 3, pp. 352–363, May 2004.

[16] L. Serrao, S. Onori, and G. Rizzoni, "ECMS as a realization of Pontryagin's minimum principle for HEV control," in *Proc. Amer. Control Conf.*, 2009, pp. 3964–3969.

[17] C. Musardo, G. Rizzoni, Y. Guezennec, and B. Staccia, "A-ECMS: An adaptive algorithm for hybrid electric vehicle energy management," *Eur. J. Control*, vol. 11, nos. 4–5, pp. 509–524, 2005.

[18] B. Gu and G. Rizzoni, "An adaptive algorithm for hybrid electric vehicle energy management based on driving pattern recognition," in *Proc. ASME Int. Mech. Eng. Congr. Expo., Dyn. Syst. Control A B*, Jan. 2006, pp. 249–258.

[19] J. T. B. A. Kessels, M. W. T. Koot, P. P. J. van den Bosch, and D. B. Kok, "Online energy management for hybrid electric vehicles," *IEEE Trans. Veh. Technol.*, vol. 57, no. 6, pp. 3428–3440, Nov. 2008.

[20] S.-I. Jeon, S.-T. Jo, Y.-I. Park, and J.-M. Lee, "Multi-mode driving control of a parallel hybrid electric vehicle using driving pattern recognition," *J. Dyn. Syst., Meas., Control*, vol. 124, no. 1, pp. 141–149, Mar. 2002.

[21] S. Onori, L. Serrao, and G. Rizzoni, "Adaptive equivalent consumption minimization strategy for hybrid electric vehicles," in *Proc. ASME Dyn. Syst. Control Conf.*, Jan. 2010, pp. 499–505.

[22] F. Lacandia, L. Tribioli, S. Onori, and G. Rizzoni, "Adaptive energy management strategy calibration in PHEVs based on a sensitivity study," *SAE Int. J. Alternative Powertrains*, vol. 2, no. 3, pp. 443–455, Sep. 2013.

[23] P. Tulpule, V. Marano, and G. Rizzoni, "Energy management for plug-in hybrid electric vehicles using equivalent consumption minimisation strategy," *Int. J. Electr. Hybrid Vehicles*, vol. 2, no. 4, pp. 329–350, Jan. 2010.

[24] P. Khayyer, J. Wollaeger, S. Onori, V. Marano, U. Ozguner, and G. Rizzoni, "Analysis of impact factors for plug-in hybrid electric vehicles energy management," in *Proc. 15th Int. IEEE Conf. Intell. Transp. Syst.*, Sep. 2012, pp. 1061–1066.

[25] D. F. Opila, X. Wang, R. McGee, R. B. Gillespie, J. A. Cook, and J. W. Grizzle, "An energy management controller to optimally trade off fuel economy and drivability for hybrid vehicles," *IEEE Trans. Control Syst. Technol.*, vol. 20, no. 6, pp. 1490–1505, Nov. 2012.

[26] M. Khodabakhshian, L. Feng, and J. Wikander, "Optimization of gear shifting and torque split for improved fuel efficiency and drivability of HEVs," SAE Tech. Paper 2013-01-1461, 2013.

[27] E. Galvagno, M. Velardocchia, and A. Vigliani, "Dynamic and kinematic model of a dual clutch transmission," *Mechanism Mach. Theory*, vol. 46, no. 6, pp. 794–805, Jun. 2011.

[28] E. Galvagno, G. R. Guercioni, and A. Vigliani, "Sensitivity analysis of the design parameters of a dual-clutch transmission focused on NVH performance," SAE Tech. Paper 2016-01-1127, 2016.

[29] Z. Song, W. Guangqiang, and Z. Songlin, "Study on the energy management strategy of DCT-based series-parallel PHEV," in *Proc. Int. Conf. Comput., Control Ind. Eng.*, vol. 1, 2010, pp. 25–29.

[30] E. Galvagno, G. R. Guercioni, G. Rizzoni, M. Velardocchia, and A. Vigliani, "Effect of engine start and clutch slip losses on the energy management problem of a hybrid DCT powertrain," *Int. J. Automot. Technol.*, vol. 21, no. 4, pp. 953–969, 2020, doi: 10.1177/s12239-020- 0091-y.

[31] G. Li and D. Görges, "Optimal integrated energy management and shift control in parallel hybrid electric vehicles with dual-clutch transmission," *Proc. Inst. Mech. Eng. D, J. Automobile Eng.*, vol. 234, nos. 2–3, pp. 599–609, Feb. 2020.

[32] O. Sundstrom, P. Soltic, and L. Guzzella, "A transmission-actuated energy-management strategy," *IEEE Trans. Veh. Technol.*, vol. 59, no. 1, pp. 84–92, Jan. 2010.

[33] V. Ngo, T. Hofman, M. Steinbuch, and A. Serrarens, "Effect of gear shift and engine start losses on energy management strategies for hybrid electric vehicles," *Int. J. Powertrains*, vol. 4, no. 2, pp. 141–162, 2015.

[34] L. Engbroks, P. Knappe, D. Goerke., S. Schmiedler, "Energetic costs of ICE starts in (P)HEV—Experimental evaluation and its influence on optimization based energy management strategies," SAE Tech. Paper 2019-240203, 2019, doi: 10.4271/2019-24-0203.

[35] L. Guzzella and A. Sciarretta, *Vehicle Propulsion Systems: Introduction to Modelling and Optimization*, 3rd ed. Berlin, Germany: Springer-Verlag, 2013.

[36] M. Tutuianu, P. Bonnel, B. Ciuffo, T. Haniu, N. Ichikawa, A. Marotta, J. Pavlovic, and H. Steven, "Development of the world-wide harmonized light duty test cycle (WLTC) and a possible pathway for its introduction in the European legislation," *Transp. Res. D, Transp. Environ.*, vol. 40, pp. 61–75, Oct. 2015.

[37] E. Galvagno, A. Tota, M. Velardocchia, and A. Vigliani, "Enhancing transmission NVH performance through powertrain control integration with active braking system," SAE Tech. Paper 2017-01-1778, 2017.

[38] A. Tota, E. Galvagno, M. Velardocchia, and A. Vigliani, "Passenger car active braking system: Model and experimental validation (Part I)," *Proc. Inst. Mech. Eng. C, J. Mech. Eng. Sci.*, vol. 232, no. 4, pp. 585–594, Feb. 2018.

[39] A. Tota, E. Galvagno, M. Velardocchia, and A. Vigliani, "Passenger car active braking system: Pressure control design and experimental results (part II)," *Proc. Inst. Mech. Eng. C, J. Mech. Eng. Sci.*, vol. 232, no. 5, pp. 786–798, Mar. 2018.

[40] G. Paganelli, S. Delprat, T. M. Guerra, J. Rimaux, and J. J. Santin, "Equivalent consumption minimization strategy for parallel hybrid powertrains," in *Proc. Veh. Technol. Conf. IEEE 55th Veh. Technol. Conf. VTC Spring*, vol. 4, May 2002, pp. 2076–2081.

[41] G. Paganelli, G. Ercole, A. Brahma, Y. Guezennec, and G. Rizzoni, "A general formulation for the instantaneous control of the power split in charge-sustaining hybrid electric vehicles," in *Proc. 5th Int. Symp. Adv. Vehicle Control*, 2000, pp. 73–80.

[42] N. Kim and A. Rousseau, "Sufficient conditions of optimal control based on Pontryagin's minimum principle for use in hybrid electric vehicles," *Proc. Inst. Mech. Eng. D, J. Automobile Eng.*, vol. 226, no. 9, pp. 1160–1170, Sep. 2012.

[43] G. Paganelli, "General supervisory control policy for the energy optimization of charge-sustaining hybrid electric vehicles," *JSAE Rev.*, vol. 22, no. 4, pp. 511–518, Oct. 2001.

[44] W. Enang and C. Bannister, "Robust proportional ECMS control of a parallel hybrid electric vehicle," *Proc. Inst. Mech. Eng. D, J. Automobile Eng.*, vol. 231, no. 1, pp. 99–119, Jan. 2017.

[45] L. Tang, "Optimal energy management strategy for hybrid electric vehicles with consideration of battery life," Ph.D. dissertation, Dept. Mech. Eng., Ohio State Univ., Columbus, OH, USA, 2017.

GUIDO RICARDO GUERCIONI was born in Caracas, Venezuela, in 1990. He received the degree in mechanical engineering from the Universidad Simón Bolívar, Caracas, in 2014, and the Ph.D. degree in mechanical engineering from Politecnico di Torino, Turin, Italy, in 2018.

From 2016 to 2017, he was a Visiting Scholar with the Center for Automotive Research (CAR), Ohio State University, Columbus, OH, USA. His research interests include torsional vibration analysis, powertrain systems modeling and development, transmission systems analysis, e.g., dual-clutch transmissions (DCTs) and automated manual transmissions (AMTs), and hybrid electric vehicles (HEVs) energy management strategies (EMSs).

Dr. Guercioni has been a member of the Society of Automotive Engineers (SAE). He was awarded the Scholarship to pursue his M.S. degree.

ENRICO GALVAGNO was born in Fossano, Italy, in 1979. He received the degree (Hons.) in mechanical engineering and the Ph.D. degree in applied mechanics from the Politecnico di Torino (PoliTo), in 2004 and 2008, respectively.

After his Ph.D. degree, he continued his research activity as a Research Assistant with the Department of Mechanical and Aerospace Engineering (DIMEAS), PoliTo, mainly in the fields of modeling, simulation, testing, and control of automotive transmission systems. From 2015 to 2017, he has served as a Researcher with DIMEAS, where he has been an Associate Professor in applied mechanics, since 2018. He is also a member of the Vehicle Dynamics and Active Safety Systems Research Team, PoliTo.

Dr. Galvagno is a member of the Steering Committee of the Center for Automotive Research and Sustainable Mobility (CARS), PoliTo. In 2020, he joined the Technical Committee for Engines and Powertrains of IFFTOMM.

ANTONIO TOTA received the M.S. and Ph.D. degrees in mechanical engineering from the Politecnico di Torino, Italy, in 2013 and 2017, respectively.

From 2018 to 2019, he was a Research Fellow in advance vehicle engineering with the University of Surrey, Guildford, U.K. Since 2019, he has been a Research Assistant with the Department of Mechanical and Aerospace Engineering, Politecnico di Torino. He is also a member of the Vehicle Dynamics and Active Safety Systems Research Team, Politecnico di Torino. His main research interests include vehicle dynamics control and autonomous driving for on-road and off-road applications.

Dr. Tota is a member of the Society of Automotive Engineers (SAE).

ALESSANDRO VIGLIANI (Member, IEEE) received the M.S. degree in aerospace engineering and the Ph.D. degree in mechanical engineering from the Politecnico di Torino, Italy, in 1992 and 1996, respectively.

From 1999 to 2009, he was a Research Assistant with the Department of Mechanical Engineering, Politecnico di Torino. Since 2010, he has been an Associate Professor with the Department of Mechanical and Aerospace Engineering, Politecnico di Torino. He is also a member of the Vehicle Dynamics and Active Safety Systems Research Team, Politecnico di Torino. His research interests include rotordynamics, vehicle dynamics, automotive drivelines, and vibrations.

Dr. Vigliani is a member of the Society of Automotive Engineers (SAE).